ADVANCED FUEL RESEARCH
87 Church Street
East Hartford, CT 06108-3742
Telephone (860) 528-9806
Fax (860) 528-0648
www.AFRInc.com

PHASE I
FINAL REPORT

"*Infrared Spectrometer on a Chip*"

Air Force Contract No: F49620-97-C-0050

Report No.: (0002AA)
Report Period: 15 Aug, 1997 – 14 May, 1998
Contract Period: August 15, 1997 – May 14, 1998

Prepared For:
Department of the Air Force
Air Force Office of Scientific Research (AFMC)

Prepared By:
Dr. David G. Hamblen, Principal Investigator

Advanced Fuel Research, Inc.
87 Church Street
East Hartford, CT 06108

AFR Project No.: 526048

Distribution Statement A:
"Approved For Public Release; Distribution Is Unlimited."

August 17, 1998

INFRARED SPECTROMETER ON A CHIP

TABLE OF CONTENTS

TABLE OF FIGURES

1.0 INTRODUCTION

Infrared spectroscopy has long been recognized as an excellent tool for sensing and monitoring chemical species and thermal signatures. Applications appear in the semiconductor, utility, petroleum, chemical, transportation, medical and environmental industries, in R&D and in the military. the drawback is that infrared spectrometers and detectors are complex systems which are expensive ($20,000 or more) and involve moving mechanical parts which must be maintained in careful alignment. There is a need for low-cost (less than a few hundred dollars) devices which can be used in these applications.

the innovation in this program is to combine two innovative micro-machining technologies presently under development to fabricate a low cost spectrometer on a single opto-electronic silicon chip.

In a Department of Energy funded program[1], Advanced Fuel Research, Inc. (AFR) began development of a micro-machined graded interference filter (GIF) on a silicon chip, a device which provides the spectral information, but which requires an array of detectors to be useful as a spectrometer. Raytheon/TI Systems is developing a low-cost uncooled amorphous silicon microbolometer array technology [2,3] which is ideally suited to this application. the advantages of this combination are: 1) that the GIF array etalons provide the throughput advantages long recognized for Fourier Transform Infrared (FT-IR) (approximately half the infrared energy is incident on the entire detector array at all resolutions, as opposed to only the energy in a narrow filter bandpass for a dispersive or filter spectrometer); 2) the microbolometer array provides the detectors required for the GIF using a simple rugged low-cost technology; 3) all components can be fabricated using standard silicon foundry techniques, including most of the readout electronics; and 4) since silicon is the material of choice for both the etalon and bolometer arrays, the mating of the two should be straightforward.

In this program, the goal was to combine AFR's silicon etalon array (GIF) technology with TI's uncooled micro-bolometer array to test the capability of these technologies as an infrared spectrometer. In Phase I, the approach was to fabricate the etalon array and bolometer array separately in a low resolution configuration and assemble them together with the appropriate optics to demonstrate the resolution and sensitivity of the spectrometer. In Phase II, we will continue this effort, increasing the resolution, and consider ways to integrate both the etalon and detectors arrays on a single chip or module using Raytheon's latest integrated microbolometer/readout array, and to extend the technology to imaging spectrometry.

the team of AFR, and Raytheon/TI Systems, provides a strong research capability to address the questions in this proposal. AFR has long been a leader in infrared spectroscopic techniques, especially in Fourier Transform Infrared spectroscopy, leading to a spin-off company, On-Line Technologies, Inc., formed in 1991 for the purpose of commercializing these techniques through sales of FT-IR spectrometers and applications, especially in the semiconductor industry. AFR and On-Line have over 13 patents directly related to IR spectroscopy and applications, including one on the graded interference filter [4] which represents part of AFR's contribution to this proposal. Raytheon's expertise in electronics, silicon foundry techniques, and integration of electronics with microbolometers makes this an exciting opportunity to capitalize on a market for gas sensors. As an indicator of the commercial potential of these concepts, Raytheon/TI Systems has invested over $2 million to date on a-Si microbolometer technology including this project, and will spend over $700,000 this year on commercialization of this technology. They are currently transitioning to prototype

production for a-Si microbolometers. A Phase III commitment for the Phase III program has been obtained from On-Line Technologies, Inc.

2.0 PROGRAM OBJECTIVES

2.1. Overall Objectives

the near-term (Phase I) objective of the program is to demonstrate the feasibility of the spectrometer on chip by mating the two array chips (GIF etalons and detectors) together. the long-term goal (Phases II and III) will be to develop an imaging spectrometer on a chip, using two-dimensional arrays, with one dimension used for spectral information, and the other for spatial (1D) information, with integrated sensor, etalon, and readout electronics for scanning an image.

Phase I was carried out in four Tasks:

Task I. Design and Fabricate Etalon Array to Integrate with Bolometer Array (AFR).

To fabricate an etalon array with the appropriate geometry to mate with TI's 64 channel bolometer array.

Task II. Fabricate Bolometer Array (Texas Instruments)

To fabricate and deliver to AFR two 64-channel amorphous silicon microbolometer arrays.

Task III. Integrate Etalon and Bolometer Arrays

To construct and assemble the optics, gas cell, etalon array, and microbolometer array into a working spectrometer.

Task IV. Test and Evaluate System

Using several IR absorbing gases demonstrate the sensitivity and resolution of the spectrometer. Compare spectrometer with competing technologies with regard to cost and range of application. Consider methods and possibility for integrating the two arrays on a single silicon wafer.

3.0 PROGRESS REPORTS AND RESULTS

3.1 Introduction

In order to take better advantage of the current state of development in both the microbolometer arrays and the etalon arrays, we decided to change from the 64 channel to a 25-channel format for the microbolometers. In discussions with TI (now Raytheon/TI systems) it was determined that for the initial tests it would be better to use a smaller number of etalon windows. the individual pixels in the 78x256 array can be connected in series internally into channels when the microbolometer arrays are fabricated, and the channels can be either monitored individually or connected externally in parallel when used. Since the internal series connection provides greater signal strength, and since an odd number of channels per superpixel provides a better pinout on the package, it was decided to use 25 superpixels of 5 channels each in the bolometer array.

3.2 Task I. Design and Fabricate Etalon Array to Integrate with Bolometer Array

To fabricate an etalon array with the appropriate geometry to mate with TI's 64-channel bolometer array.

the fabrication of the etalons consisted of three steps:

1. Design and preparation of photomasks
2. Patterning the silicon wafers with the etalon array.
3. Etching the etalons to the desired thicknesses.

3.2.1 Design and Preparation of Photomasks

As mentioned above, it was decided to connect internally the pixels from Raytheon/TI's 256x78-pixel microbolometer array into 25 channels of 10x78 pixels.

To start, we obtained the layout masks for the bolometer array from Raytheon/TI with the detailed dimensions. the pixels are arranged in 256 columns of 78 pixels each. the columns are internally interconnected into 128 pairs. Fig. 1 (page 22) shows the entire bolometer. the working copy of this figure, with the dimensions, is about 1 m long. Shown in Fig. 2 (page 23) is a closer look at 16 of these pairs of columns. Fig. 3 (page 24) shows a detail view of 4 pixels from one of these column pairs. For this program, these column pairs are interconnected in groups of 5, providing 25 channels of 10x78 pixels. This leaves 6 unused columns.

the etalon arrays for this program involved a minor scaling up from our previous work, since all the previous work had been done with 11mm square pieces of silicon, and this effort requires 17 mm squares. In order to proceed and to train a new employee in the process, we started with an array of 5 etalons to cover the 25 bolometer superpixels. We generated the CAD file drawings, the negative paper masks (switching from 8.5x11 inch paper to 11x17 inch paper), and the photomasks. We modified the photoresist spinner to accept the larger samples. We prepared both paper and photomasks for 1x5 and 1x8 etalons to mate with the TI bolometer array.

One area of concern is the strength of a silicon window, given by

$$p \propto m \cdot \left(\frac{t}{d}\right)^2 \tag{8}$$

where m is the modulus of rupture (~9000psi for SI), t is the thickness, d is the dimension (width or diameter of the window, and p is the breaking pressure. the constant of proportionality relating pressure is of order unity, and depends on whether the window is circular, rectangular, clamped or unclamped, etc.. For the one mm square etalon used in Phase I, we have a t/d ratio of about 10^{-3}, providing a strength of about 0.01psi, which is very weak, indeed. When we reduce the etalon size down to the pixel size, the rupture pressure is about 4 psi, or a quarter of an atmosphere. However, even that would be for an isolated etalon. In the work in Phase I, we designed the etalons to have a support bar of full wafer thickness between each etalon. In order to leave this bar, within the design constraints of the superpixel size, we have determined that the parameters in Table I (page 55) are the only possibilities. the bolometer array in Phase I is arranged into superpixels of 4x78 pixels, which in turn are wired into channels. In Phase I, we chose 25 superpixels per channel because 1) an odd number is required in order to have the microbolometer leads come out of the package in a convenient

geometry for wiring, and 2) 25 channels wasted only 3 of the 128 superpixels in the array, while providing for 5 superpixels wired in series internally in the array, which gives a reasonable output voltage. the constraints on the etalon array, then, are 1) the bolometer array is internally wired to provide 25 channels of 5 superpixels each; 2) the silicon 111 plane at 54.7° means that the etalon pit has sloping sides; 3) We want each etalon to illuminate the same number of active channels.

As can be seen from Table I, we are wasting a significant fraction of the active area of the bolometer array with this geometry.

For Phase II, we can have the silicon wafers prepared with the desired thin nitride coating on both sides; the silicon wafer can be the thickness of the thickest etalon, and any additionally required support structure can be bonded to the thin wafer. This procedure would allow the support structure to be designed without necessarily being limited by the <111> plane of the Si. For example, the support structure could be fabricated using any of several techniques, such as reactive ion etching, or various laser methods. Such improvements in fabrication are almost certainly required in order to achieve the fill factors to match the microbolometer array.

Table II (page 56) shows the design rules for the paper mask and photomask preparation.

Figs. 4 and 5 (pages 25 and 26) show the masks used.

3.2.2 Patterning of Etalons

We have successfully fabricated the 1x5 etalon array, demonstrating that the scale-up from our 1-cm previous experimental setup to the 2-cm setup is correct, and that the new employees were able to perform all the steps.

the patterning process sequence is shown in Table III (page 57).

Each iteration of this part of the process takes a minimum of an hour: 10 minutes to clean the wafer, 30 minutes to bake the wafer to dryness, 10 minutes to apply the photoresist and print it, 15 minutes hard bake for the photoresist, and 5-10 minutes to print through the silicon nitride. Many of these steps can be interleaved with multiple samples.

3.2.3 Etching of Etalons

Once the pattern is etched into the etalon, at this point we have a 1x5 thick etalon set: the thickest etalon is the full thickness of the starting wafer, with the remaining etalons in the array each approximately 1 μm deeper than the previous. At this point, it is necessary to thin the entire array down to the desired thickness (typically 1μm for the thinnest). This takes a total of about 90 minutes using 30 wt% KOH at 90°C.

One problem encountered early on was that when we prepared a fresh batch of the 30 wt% KOH water solution, we were unable to obtain smooth etches of the silicon. By dissolving 10 wt% of Si in the KOH (to simulate the estimated loading of the old batches) the etching once again became smooth. For the 30-90 second etches required for the initial patterning, this roughness was not a problem, but for the 90 minute etch to get to the final thickness the roughness becomes excessive. A recent publication [5] demonstrates that the use of ultrasound agitation to remove the bubbles which form on the silicon greatly improves the smoothness. For our purposes, at least with the etalon configuration

used in Phase I, however, the etalons are too fragile to tolerate any ultrasound or even vigorous shaking.

We have prepared a number of the 1x5 etalon arrays and tested them. Several are of excellent quality. These are all etched to a thickness increment of about 12 μm. This is done in several steps: first the sequence of photolithography to pattern and etch each etalon to the 1μm spacing through the silicon nitride mask, followed by patterning the backside nitride to expose the entire etalon area for further thinning. We found that the backside nitride can be patterned by using black vinyl electrical tape to mask the areas which shouldn't be etched by the 49 wt% HF at room temperature. Not all brands of tape work, however. We found one that does work is Tartan 1710 by 3M Office Products. (the more commonly available 3M #33 or #88 tapes don't work). the approach is to remove 90% of the remaining thickness in any one step in order to avoid overshooting the goal. (Ten percent variations in etch rate are common, due to temperature variations). the entire etalon array is thus thinned from about 400μm to 40μm in one step. the etalons are measured using FT-IR to determine how much additional etching is required. the next steps will be to thin to 12μm, and then to the final 1μm. Shown in Figs 6-8 (pages 27-29) are the transmission fringe spectra for three etalon arrays after the second etch.

A second approach pursued in this Task was to have an etalon prepared by Revise, Inc using their halogen-based laser etching technique. They are able to obtain 1-5° wall angles, with 30nm surface roughness on the pit bottoms. These specifications should be ideal for our application, and would allow for much better fill factors than those shown in Table I. Preliminary measurements on two etalons prepared by Revise show some promise. A larger etalon of 1x1 mm gave a measured depth of 40 μm with marginally adequate finesse. This etalon was etched using a higher power fast etch which should be somewhat rougher than optimum. A second 20x20μm hole was too small to measure with our present setup. This promising option should be pursued further. Figure 9 (page 30) shows these patterns, and Fig. 10 (page 31) shows the transmission spectrum obtained using the larger hole.

3.3 Task II. Fabricate Bolometer Array

To fabricate and deliver to AFR two 64 channel amorphous silicon microbolometer arrays.

As discussed in Task I, early in the program, Raytheon/TI provided detailed layouts for the bolometer array so that the etalon design could proceed. Raytheon/TI modified the masks to provide a 25 channel microbolometer array and delivered two of these, together with a socket fixture for mounting the bolometers. Fig. 11 (page 32) shows a photo-micrograph of these pixels, and Fig. 12 (page 32) shows the package including the vacuum lid. These were packaged with an IR-transparent Ge lid (Fig. 13, page 33) In addition, Raytheon/TI supplied the schematics for the electronics for the bias and readout circuits.

Tables IV and V (pages 58-59) show the specifications for the two delivered bolometers.

3.4 Task III. Integrate Etalon and Bolometer Arrays

To construct and assemble the optics, gas cell, etalon array, and microbolometer array into a working spectrometer.

In this Task, we assembled a spectrometer which can double as a test fixture for the etalons and bolometers. In addition to the mechanical and optical design aspects of this, it is also necessary to

completely characterize the etalon optical transmission properties, since the exact transform needed to obtain an infrared spectrum from the bolometer readings depends on these properties. Thus this Task has 2 subtasks:

- FT-IR characterization of etalons
- Design and Construction of Spectrometer/Test fixture

3.4.1 FT-IR Characterization of Etalons

3.4.1.1 Background (This section is based on the same section from the Phase I proposal)

the basic idea behind the graded interference filter (GIF) is similar to Fourier Transform Infrared Spectroscopy (FT-IR) in that the IR spectrum is modulated by a series of periodic intensity envelopes, the spectrum is recovered by a mathematical transform, and they are both high optical throughput methods. In the case of conventional FT-IR, each wavelength is modulated in time by a unique cosinusoidal envelope using a moving mirror Michelson interferometer, and these modulated waveforms are added together and detected by a single detector. the resulting time sequence is the interferogram. Because the modulation is a cosine function, the original spectrum can be recovered by a straightforward inverse Fourier transform. In the case of the GIF, a series of etalons is used to modulate the incident spectrum with a wavelength-periodic transmission function defined by the fringe pattern of the etalon. Using a sufficient number of etalons, each with its own detector, the sequence of measurements from each etalon again provides an interferogram which can be mathematically transformed to recover the original spectrum. In both cases, a significant fraction (~ 1/3 to 1/2) of the light incident on the spectrometer is detected and used to measure the spectrum. This is in contrast to a diffraction or filter spectrometer where only the very narrow scanned bandpass is incident on the detector during the measurement of each wavelength. This large light throughput is significant since directly improves the signal-to-noise for a given spectral measurement time.

Our design is based on the Fabry-Perot (FP) interferometer, in which each etalon receives the same IR beam [4,6]. Each FP etalon has a unique thickness and hence etalon fringe pattern. the fringe-modulated IR is passed to an array of broad-band IR detectors (such as bolometers) [7,8], in one-to-one correspondence with the etalon array. the detectors integrate the spectral bandwidth, and the array of output signals can be made to correspond to an interferogram of the incident IR spectrum [4-8]. This interferogram together with the knowledge of the detailed fringe patterns of the etalon array is then transformed to recover the original spectrum. Low-doped or cryogenic silicon wafers are suitably transparent over much of the IR spectrum, and the high index of refraction of silicon assists in some aspects of the design of our device. We have run detailed simulations of the system, which have revealed a number of design features. For example, the spectral fidelity of the entire spectrometer is improved by *not* using high-finesse etalons, a factor which simplifies fabrication. the total array area need not be more than a few square centimeters [4]. A bandpass filter is required to eliminate aliasing from spectral features outside the region of interest.

the optical function of the etalon array is similar to that of a single etalon in step-scan mode, but the array performs all interferometry at each step position simultaneous in time and parallel in space [9,10]. Simulations of models with 256 etalon elements indicate that excellent calculated spectra (inverse transform) can be obtained for realistic fabrication design choices. the choice of the series of etalon-plate thicknesses across the array is critical. Essentially, the thinnest plate must have fringes wide enough that one fringe will span the IR-spectral bandwidth of interest, i.e., the series fundamental in the transformed representation, and each subsequent etalon is an integer multiple of the first, adding

one more fringe in the bandpass, analogous to a Fourier series. Note that this implies that all the resolution elements are in the bandpass of interest, in contrast to FT-IR, where the resolution is spread over the full zero to maximum frequency. High finesse results in fringes that are so narrow that some spectral portions of the bandwidth are not well sampled by any of the etalons in a finite number of array elements. Figure 14 (page 34) illustrates an example of transmission fringes for an array of four etalons for use in the 600 to 750 cm^{-1} band. the transmission $T(n)$ through an etalon is given by Airy's formula [11], which is of the form:

$$T(\nu) \propto \{1+F(\nu) \sin^2 (\pi n d \nu)\}^{-2} \qquad (1)$$

To gain insight into the effect of design choices, such as the series of thicknesses and the finesse, we have run numerous simulations. As an example, for the IR band of 2000 to 4000 cm^{-1}, a 256-element array will have the computed transform spectrum and the original spectrum within ~1% for an incident Lorentzian line with FWHM of 25 cm^{-1} as shown in Figure 15 (page 35). Figure 15 shows the results for simulations for 16, 32, and 64 etalons. For an array of 8 etalons, the two peaks at 2400 and 2600 cm^{-1} are not resolved, but they are distinct from the peak at 3500 cm^{-1}. As can be seen from Fig. 15, the 16 element array barely resolves the first two peaks, and with 64 elements, the resolution is excellent, and P_i is within 8% of I_i. With 128 elements, the accuracy is within 1%. Incidentally, there is no requirement that the number of elements be powers of 2.

We have found that techniques such as apodization and Fourier filtering of the interferogram can improve on the overall transform quality by minimizing the usual artifacts due to aliasing and spectrum truncation. Recently, while simulating some of the actual fabricated etalons which have only approximately the correct thicknesses, we observed that the aliasing problem is greatly improved by having etalons which are slightly off from the integer multiples. Table VI (page **60**) shows the etalon thicknesses used.

Fig. 16a (page 36) shows the transmission from the etalons with thicknesses listed in Table VI as "Target Size". These are the same ones shown in Fig. 14, but over a different spectral range. Note that, in contrast to the data in Fig. 14, the fringes do not start at 1.0 at the start of the bandpass. This is because this is an etalon set designed for the range 600 to 750cm^{-1}, being used in the range of 800-950 cm^{-1}. Fig. 16b (page 36) shows the first four etalon transmission spectra for the thicknesses shown as "Actual Size" in Table VI. Fig 16c (page 36 shows a spectrum with the computed spectrum, for the "Target" etalon set, while Fig. 16d (page 36) shows the same curves for the "Actual" etalon set. the peak near 925 cm^{-1} is an artifact due to aliasing. By varying the first few etalon thicknesses, the aliasing is greatly diminished, as shown in Fig 16d. the tradeoff appears to be increased noise (or decreased signal/noise ratio) in the proper bandpass (600-750cm^{-1}) in exchange for improved performance at all frequencies. the overall usefulness of the spectrometer is improved by breaking the symmetry of the etalon set. Other simulations using this type of etalon set demonstrate that as long no two etalons are identical in thickness, transform errors are not a problem. In particular, the two etalon thicknesses can be within 5% of each other before errors in transform spectra increases by 5% over the ideal case.

the tradeoffs between the FT-IR and the GIF spectrometers are that the FT-IR requires only a single detector, and the modulator (a Michelson interferometer) provides purely sinusoidal modulation, but requires highly accurate, delicate and costly moving mirrors; while the GIF system requires one detector for each etalon, and the modulation functions contain undesirable higher order harmonics, but has no moving parts.

In addition to the significant thoughput advantage that all transform spectrometers have over filter or dispersion spectrometers, there are several signal losses and noise sources which affect FT-IR but do **not** affect GIF:

1) Fewer optical elements in the optical path

2) Large dynamic range required by the FT-IR by virtue of the centerburst feature. the GIF has an even spread of energy across the detector elements, and they all have similar dynamic range requirements. This can potentially lead to about a ten-fold SNR improvement.

3) Sampling errors can occur if the FT-IR mirror velocity is not accurately maintained. This puts a large burden on the opto-mechanical design and construction, and is a major factor in the cost of an FT-IR.

Based on the simulations, the design properties of the etalon array are as follows:
There is one open hole (totally transparent) etalon to serve as a reference.
the thinnest etalon has a full half-fringe over the bandpass required.
Subsequent etalons are integer multiples of the thinnest (analogous to Fourier series). Each such etalon divides the bandpass into resolution elements. Thus N etalons divide the bandpass into N resolution elements (resolution = 1/N bandpass).
(Tentative) These etalons should not be exact integer multiples of each other, in order to allow use over a continuum of frequencies.
the etalon/detector array requires a bandpass filter over the entire array to prevent aliasing.

3.4.1.2 - Basic Algorithm for GIF transform - *(the initial derivation of the Equations in this Section was done on the DOE Phase II program[1].)* In this section, we derive the algorithm for the GIF transform in more detail than the discussion above in order to introduce the Fourier filtering in a natural way, and to make clear what information needs to be measured as part of the etalon characterization, and how this information is used in practice. A block diagram of the problem we need to solve is shown in Fig 17. We have a source, $E(\nu)$, several transmission blocks (filter, etalons, sample, various path corrections), τ, and a detector array, $R(i,\nu)$. the spectrum as measured through this system is given by:

$$S(i,\nu) = E(\nu) * \tau_p(\nu) * \tau_f(\nu) * \tau_s(\nu) * \tau_e(i,\nu) * R(i,\nu) \qquad i = 0, M-1 \qquad (1)$$

In practice, we measure the ac voltage produced by each detector as the energy source, $E(\nu)$ is modulated by a chopper. This voltage is proportional to $S(i,\nu)$ integrated over all frequencies, ν. For testing and characterization of the etalons and detectors, we can measure each of the factors in Eq 1 using an FT-IR. Performing the integral, and grouping the factors into known and unknown quantities, we have

$$S_i = \int_{all\_frequencies} \left[E(\nu) * \tau_p(\nu) * \tau_f(\nu) * \tau_s(\nu) * R_0(\nu)\right] * \left[\frac{\tau_i(\nu) * R_i(\nu)}{R_0(\nu)}\right] d\nu \qquad i = 0, M-1 \quad (2)$$

the quantities in the first square bracket are all unknowns, while S_i, and the quantities in the second set of brackets are all measurable properties of the etalon/detector array. the factor $R_0(\nu)$ is the detector response of the 0^{th} detector, which has no etalon. Normalizing the factors by this quantity should help to minimize the effects of detector drift. Note that this particular partitioning is not unique, and other partitions may be more useful for different applications. the quantity in the first bracket is the usual

single beam energy spectrum measured in FT-IR, and once we have extracted this quantity, we have reduced the problem to the usual FT-IR analysis. In particular, we can measure this quantity both with and without a sample, and ratio the energy spectra to obtain the transmission of the sample. To invert this equation, we use the standard trick of expanding the quantity in the first bracket into a basis set (for example, a fourier series, or any other convenient basis set). Define

$$e(\nu) = E(\nu) * \tau_p(\nu) * \tau_f(\nu) * \tau_s(\nu) * R_0(\nu) \qquad (3)$$

and

$$T_i(\nu) = \frac{\tau_i(\nu) * R_i(\nu)}{R_0(\nu)} \qquad i = 0, M-1 \qquad (4)$$

and assume that the etalon spectra are linearly independent, and therefore span the vector space. We can then define a basis set as:

$$e(\nu) = \sum_{k=0}^{M-1} c_k \cdot t_k(\nu) \qquad (5)$$

where the $t_k(\nu)$ are the basis vectors, and the c_k are the coefficients. If this is a Fourier set, then the c_k are the usual interferogram. It is equally valid to use the etalon spectra themselves as the basis set. Substituting Eqs. 3 and 5 into 2, and interchanging the order of summation and integration, we have

$$S_i = \sum_k c_k \cdot \int_\nu t_k(\nu) \cdot T_i(\nu) d\nu \qquad (6)$$

Since, the basis set must have the same number of vectors as the number of etalons, including the empty etalon, the integral is a square array, Z_{kj}, and if the etalon spectra are linearly independent, as well as the basis set being linearly independent, then this square matrix will have an inverse, Z^{-1}_{ik}. Furthermore, this matrix contains only known quantities: the etalon spectra perhaps scaled by the detector responsivities, and the basis set of spectra. As indicated in Eq. 6, each element in the matrix is the inner product of two spectra, an etalon spectrum and a basis spectrum (which may be the etalon spectra themselves).
Using this inverse matrix,

$$c_k = \sum Z^{-1}_{ki} \cdot S_i \qquad (7)$$

Substituting Eq. 7 back into Eq 5 provides the desired single-beam energy spectrum.

In summary, then, the procedure is

- Measure $T_i(\nu)$ as part of the characterization of the instruments. This need only be done once, and assumes that the entire etalon/detector array is uniformly illuminated by the source, and that the responsivities do not drift.
- Define a basis set, $t_i(\nu)$, to use in the inverse transform. We have found the best results are obtained by using the etalon transmissions themselves.
- Form the transform matrix, $Z_{ij} = \sum T_{ik} T_{kj}$ and its inverse Z_{ij}^{-1} as indicated above. These matrices are an integral part of the spectrometer, just as the matrices of cosine functions are an implicit part of an FT-IR.

At this point one has the basic information one needs to use the spectrometer. the measurement sequence is then:

- With no sample in place, measure all the bolometer signals, S_i^B, the Background signal.
- With a sample in place, again measure all the bolometer signals, S_j^S, the Sample signal.
- Calculate the "interferograms", c_i^B and c_j^S, using Eq. 7. and the known Z_{ij}^{-1}.
- Calculate the single beam energy spectra, $e^B(\nu)$ and $e^S(\nu)$, using Eq. 5. and the known t_i's.
- Calculate the sample transmission spectrum, $\tau(\nu)$, as the ratio of the sample/background single beam spectra.

3.4.1.3 - Characterization and Measurements of 1x5 Etalons

During the course of this program numerous wafers were prepared to test various aspects of the etching and fabrication process, 8 of which resulted in potentially useable etalon sets. the first two sets of 1x5 etalons were thinned to nominal thicknesses of (9,11,13,15,16 μm) before being broken in handling in attempting to thin them down to 3 μm. the next batch of 6 sets of 1x5 etalons were all thinned to the 60 μm level. the first one (DGH01) of these had only 4 etalons, due to a misalignment of the mask, and fractured with gentle shaking while cleaning for further thinning. It had approximate thicknesses of (7, 9, 11, 12 μm). the thinnest etalons on the next two (DGH02 and DGH03) were etched through in thinning to the next level. the last three (DGH04, DGH05, and DGH06) were thinned to minimum thicknesses of 12 μm, and in the interest of not destroying the last available etalons, it was decided to use them at that thickness and demonstrate the operation of the spectrometer with them. the "missing" thin etalons can be simulated with calculated ones.

the transmission spectra for etalon sets DGH04, DGH05, and DGH06 are shown in Figs 6-8 (page 27-29). the transmission spectra for the two bandpass filters used are shown in Fig. 18 (page 37). These spectra, together with a few simulated spectra for "missing" etalons, are the data required to use the spectrometer. In practice, the bandpass spectra cancel out of the calculation, so that the end-user can supply his/her own filter without needing detailed bandpass spectra.

3.4.2 Design of Spectrometer/Test fixture

As indicated in Fig. 17 (page 36), the spectrometer requires a source, a bandpass filter, an optional gas cell or sample holder, the etalon array, the bolometer array, and the appropriate electronics and data acquisition system. Since the detector is a bolometer, a chopper is required to modulate the light for detection. For this Task, we used one of On-Line Technologies standard sources, which is a 2mm x 4mm rectangular source. As shown in Fig. 19 (page 38), the radiation from this source is incident on a 50.8mm off-axis parabolic mirror, which provides an expanded parallel beam which passes through the optional gas cell to a second 50.8mm off-axis parabola. This second parabola brings the radiation to a focus where the chopper is located. For testing, we use a small piece of ABS plastic as a sample, also located near this focus. the light is then refocused onto the detector array. In order to ensure that the detector is properly illuminated, ray-tracing simulations were performed as indicated in Fig 19. Figs. 20-22 (pages 39-41) show the rays leaving the source, at the center aperture (chopper), and at the detector. As can be seen from Fig. 22, the source is nicely imaged onto the 3.2mm x 13.0mm detector array. the final system is shown in Fig. 23 (page 42). the etalon array and the bolometer array are mounted on XY micro-manipulators, with the etalon array as close to the bolometer array as possible.

For testing purposes, we used a simple bolometer biasing circuit provided by Raytheon/TI, a gain of 100 pre-amplifier with a 6 db/octave boost to compensate for the bolometer 6db/octave rolloff, feeding a lock-in amplifier. the 25 channels of the bolometer were connected parallel into 5 groups of 5 channels each to match with the 5 etalons.

3.5 Task IV. Test and Evaluate System

Using several IR absorbing gases and demonstrate the sensitivity and resolution of the spectrometer. Compare spectrometer with competing technologies with regard to cost and range of application. Consider methods and possibility for integrating the two arrays on a single silicon wafer.

For initial testing of the instrument, rather than using a gas cell that must have the concentrations of gases maintained stable over time in order to compare different aspects of the instrument, we used instead the two bandpass filters. the broader of the two ($783cm^{-1}$ to $1053cm^{-1}$) served as the BP filter in spectrometer to prevent aliasing. the narrower filter ($872\ cm^{-1}$ to $1000\ cm^{-1}$) served as a sample. Since we have only 5 resolution elements, this should serve as a suitably broad spectral feature. These particular bandpass filters were used because they were available in the laboratory at no cost, and are suitable for these tests.

the procedure for obtaining a spectrum, based on the discussion and algorithms in Task III, is to measure the signal from each bolometer/etalon channel with and without the sample in place. For testing purposes (to allow us to construct intermediate results and check for various path corrections), we also measured these signals with and without bandpass filters for etalon set DGH04, DGH05, and no etalon. Table VII (60) shows the raw data obtained for these cases.

In analyzing this data, we observed that there is possible clipping (vignetting) due to the insertion of the BP filters into the optical path, (thus $\tau_f(\nu) = \tau_{f,i}(\nu)$ in Eq. 2.) This means that the partitioning of the spectral components in Eqs. 3 and 4 need to be modified. If we assume that this vignetting is frequency independent, then we can write that $\tau_{f,i}(\nu) = \tau_f(\nu) * \beta_i$, where β_i is the clipping factor for each etalon. A similar observation applies to the detector sensitivities, in that we need to assume that the spectral responsivities of all bolometer channels are the same to within a scale factor, i.e. $R_i(\nu) = R_0(\nu) * \alpha_i$, where α_i is a multiplicative gain factor for each detector.

Using this in Eq. (2), we obtain

$$S_i = \int_{all\_frequencies} \left[E(\nu)*\tau_p(\nu)*\tau_f(\nu)*\tau_s(\nu)*R_0(\nu)\right]*\left[\tau_i(\nu)*\alpha_i*\beta_i\right]d\nu \qquad i = 0, M-1 \quad (2)$$

where the α and β's are the geometry/responsivity factors for the particular configuration, and the corrected signals are

$$C_i = \frac{S_i}{\alpha_i * \beta_i}$$

Choosing the center detector as R_0, and the unblocked (no BP filter) as the $\tau_f(\nu)$, we then obtain the following Table VIII (page 61) of correction factors.

With these correction factors, the corrected signals for the various cases become

Inspection of this data highlights a problem: with the chopped bolometer signals, we are interested only in the changes from a baseline with changes in sample. In taking this data with a lock-in amplifier, the last decimal place in the Tables was quite stable (i.e. the signal reproducibility was ±0.1

μV. We need the three significant figures in this measurement to be in the signal differences, not the raw signal. In order to accomplish this we need to modify the electronics to measure the raw signal from R_0, and the differences (R_i-R_0) for the other detectors.
This can be done in a number of ways, but some sort of bridge circuit will probably be best.
Sensitivity to errors or uncertainties in signal measurements is considered below with simulations.

In order to evaluate the data and the spectrometer further, we performed a number of simulations using LabView with a mix of actual and artificial spectra.

To start, we generate a file containing a set of spectra to use as a basis:

- File T5.MTX contains 8 spectra DGH0087, 98,88,97,89,90,95,91 with etalons of thicknesses (12.87, 13.72, 15.96, 16.46, 18.77, 18.62, 20.88, and 19.96).
- File T6.MTX contains 8 etalon spectra from the DOE program spectra (for thicknesses of 106.9, 110.6, 114.0, 117.6, 120.8, 124.2, 127.6, and 131.0 μm.
- File T7.mtx contains all of the T5 set plus cosine functions for Si thicknesses of 1.3, 2.6, 3.9, 5.2, 6.5, 7.8, 9.1, 10.4, and 11.7μm.

These simulations use 1). a data set of basis spectra to compute the Z-matrix in Eq. 6, and 2). either an experimental spectrum or a calculated Lorentzian peak to simulate the results of a measurement. Alternatively, a set of bolometer signals can be input to generate an experimental spectrum; or an ideal bolometer signal is generated from a spectrum. These data can then be used to perform various sensitivity analyses. In the figures that follow, Graph A is the basis set used, Graph B is the "true" spectrum and the spectrum which would be generated by an ideal measurement using the etalon/bolometer set, and graph C is the Noise from that ideal measurement. Noise, N, is defined as the rms error in the spectrum given a unit noise in the input bolometer signals. (i.e., if the noise to signal ratio for the bolometers is 1.0, then the rms error in the final spectrum is N, as shown by the "thermometer" next to Graph C on the figures.

Effect of Bandpass Filter

Using set T6.mtx, we can demonstrate several points. First, in Fig 24 (page 43), the upper left graph (highlighted as A) shows that for this etalon set, there is a repeat of the general pattern every 444 cm^{-1}, which implies that this set is suitable for a bandpass of 222 cm^{-1}. This is also reflected in the aliasing which appears in the two graphs below the first (highlighted as B and C). the spike in graph B in Fig 24 is the "sample spectrum" (not resolved). Graph "C" illustrates the noise calculation. the regions of high noise are regions which will not be accurately determined by this particular spectrometer configuration. In this particular example, the total error of 5.11 means that if we have a 1% uncertainty in our raw data, then there will be a 5.11% total uncertainty in the resulting spectrum; and it will be distributed as in Graph C. In Fig. 25 (page 44), we have set the bandpass to the proper width and starting point (222 cm^{-1} and 860 cm^{-1}) to illustrate the reconstruction of a narrow feature (graph B). Because we do not have a large enough number of resolution elements in the basis set, the feature is smeared into a sin(x)/x feature centered at the correct point. Fig. 26 (page 45)shows that this feature is properly detected anywhere within the bandpass. Fig 27 (page 46) shows that this works in any valid Nyquist zone. In this case we have changed the bandpass start to 657 cm^{-1}, but kept the bandwidth the same, and moved the feature to 705 cm^{-1} (graph B). In Fig 28, graph B (page 47), we show that broad features are not detected with this basis set, because all of the low frequency harmonics are missing. If the bandpass is changed to 85 cm^{-1} as in Fig. 29 (page 48), the total noise goes up dramatically (see graph C and the total error D). Finally, if the starting point of the bandpass

is chosen badly as in Fig. 30 (page 49), the noise is somewhat greater (for a starting point of 720 cm^{-1}, the noise figure is about 40% greater) as shown in graph C.

Effect of Missing Etalons

Analysis of the T5 data set illustrates some additional points. Using just the "high-frequency" etalons of the T5 data set as in Fig. 31, graph B (page 50), broad features cannot be described, just as in Fig 28. When set T7 is used (T5 augmented with all the low frequencies) the broad feature is completed reproduced as in Fig. 32 (page 51). A narrow feature can be detected with just set T5 (Fig. 33, graph B, page 52), but its low frequency components are missing. If we add the low frequency back in (using set T7), this narrow feature is more completely described (Fig. 34, graph B, page 53). Finally, using only the low frequency artificial components as in Fig 35 (graph B, page 54), the fit is much worse, since a narrow feature doesn't have much low frequency information.

4.0 CONCLUSIONS

the Phase I project has successfully demonstrated that the graded-interference-filter (GIF) spectrometer design concept is feasible, and that the GIF etalon arrays and the a-Si microbolometer arrays from Raytheon/TI Systems are compatible. During the course of this project, we have fabricated 11 test etalon sets, of which 3 resulted in set suitable for mating with the microbolometers. Two 256x78 microbolometer arrays were fabricated, wired internally into 25 channels of 10x78 pixels each. Both of these microbolometer arrays were tested successfully, one of them with several of the etalon sets. A spectrometer/ test fixture was assembled containing an infrared source, focusing optics, provision for a gas cell, micromanipulators for the etalon and microbolometer arrays, biasing and signal conditioning electronics, and a chopper/modulator for the bolometers.

In this project, we evaluated several designs with variations from ideal: incomplete etalon sets, etalons sets with thicknesses differing from the design target thicknesses, and the effect of differing bandpass filters in the optical path. This was done by defining and implementing the detailed algorithm for data acquisition and transform in a LabView program. This allowed the testing of actual data and simulated data, as well as combinations of both. These analyses suggest that "incomplete" etalon sets will be useful in specialized applications.

Further work is needed in improving the yield of etalons, in better signal conditioning electronics (particularly a nulling arrangement for the chopped bolometer signals), and in the area of simulations to determine the best thicknesses for the etalons. These areas can all be addressed in Phase II.

5.0 PLANS FOR PHASE II

the near-term objective in Phase I of the program was to demonstrate the feasibility of the spectrometer on chip by mating the two array chips (GIF etalons and detectors) together. the long term goal (Phases II and III) will be to develop an imaging spectrometer on a chip, using two-dimensional arrays, with one dimension used for spectral information, and the other for spatial (1D) information, with integrated sensor, etalon, and readout electronics for scanning an image.

the team of AFR and Raytheon/TI Systems, provides a strong research capability to address the questions in this proposal. AFR has long been a leader in infrared spectroscopic techniques, especially in Fourier Transform Infrared spectroscopy, leading to a spin-off company, On-Line Technologies, Inc., formed in 1991 for the purpose of commercializing these techniques through sales of FT-IR

spectrometers and applications, especially in the semiconductor industry. AFR and On-Line have over 13 patents directly related to IR spectroscopy and applications, including one on the graded interference filter [12] which represents part of AFR's contribution to this proposal. Raytheon's expertise in electronics, silicon foundry techniques, and integration of electronics with microbolometers makes this an exciting opportunity to capitalize on a market for gas sensors. As an indicator of the commercial potential of these concepts, Raytheon/TI Systems has invested over $2 million to date on a-Si microbolometer technology including this project, and will spend over $700,000 this year on commercialization of this technology. They are currently transitioning to prototype production for a-Si microbolometers. A Phase III commitment has been obtained from On-Line Technologies, Inc.

Pollution and air quality, both indoor and outdoor, are significant environmental and public health issues which continue to be of considerable public concern. Pervasive legislation and regulation in the environmental, health and worker safety areas are creating worldwide market windows for gas sensor technology to monitor air quality. Cost and gas specificity are key gas sensor requirements which are driving technology development towards multichannel gas sensor solutions. Infrared gas sensors based on infrared absorption spectroscopy offer high selectivity and sensitivity for the identification of many chemical compounds thereby offering real time multichannel gas monitoring capability for environmental gas sensor applications which include indoor air quality monitoring and continuous emissions monitoring. For these applications, infrared gas sensors must be compact, low cost, environmentally rugged and producible in high volume. the combination of AFR's GIF spectrometer with TI's uncooled amorphous silicon (a-Si) infrared microbolometer technology addresses these needs. the fabrication of both devices employ conventional silicon processing techniques compatible with low cost, high volume production in a silicon foundry. In addition, TI's microbolometer-based gas sensor approach further reduces cost by avoiding temperature stabilization and employing low cost vacuum packaging. TI's gas sensor approach also has military application in the detection and identification of chemical agents and toxic gases which are continuing and pervasive military and security threats in both battlefield and civilian environments.

AFR's present efforts are focused on developing future products which: a) have a high market potential; and b) capitalize on AFR's technology strengths. Four business focus areas have been selected: 1) Smart early warning hazard sensors for industrial and residential applications; 2) Environmental sensors for remediation activities, 3) Technology for hydrocarbon conversion and combustion, and 4) Medical diagnostic test equipment. At present, projects which enhance On-Line Technologies commercialization activities in FT-IR instrumentation are given priority. **This proposed Phase II program to combine AFR's GIF spectrometer with TI's uncooled microbolometer array to create a spectrometer without moving parts directly fits into AFR/On-Line's immediate market plans.**

Raytheon is developing a complete product line of a-Si-based microbolometer sensor and sensor system products. It is stressed that the a-Si microbolometer sensor technology is a surface micromachined Si MEMS technology approach. In addition, the a-Si microbolometer fabrication process is a *Si MEMS and Si CMOS fab-compatible process*. As such, a-Si microbolometer wafers in full scale production will be fabricated in a commercially oriented, high volume Silicon Foundry which offers the technology path for the manufacture and supply truly low cost infrared detector chips in large volumes. With regard to manufacturing, a-Si microbolometer array transition to manufacturing is presently funded by Mr. Raymond Balcerak under the DARPA ETO Infrared Focal Plane Array-Flexible Manufacturing (IRFPA/FM) Program (Contract #F33615-93-C-4320). Furthermore to

achieve low cost vacuum packaging, Raytheon is developing high volume wafer-level vacuum packaging technology under the Vacuum Packaging for MEMS Program (Contract #F30602-97-C-0127) funded by the DARPA ETO MEMS Program (Dr. Elias Towe, Dr Al Pisano).

Raytheon is targeting multiple dual use applications for a-Si microbolometer sensors and sensor system products. the strategy employed is the leverage both commercial and government marketplaces to increase volume production of a-Si microbolometer chips/packages thereby reducing chip/package cost. This strategy is identical to the approach used so successfully in the Si microelectronics industry. Raytheon's present product line development includes prototype a-Si microbolometer-based sensor engines for medical monitoring applications as well as environmental gas monitoring applications which are being developed under proprietary commercially funded programs. Prototype Raytheon environmental CO_2 and CO systems are in the field at present. Raytheon is now applying its gas sensor system technology to chemical agent sensor applications.

Under the Autonomous Networked Tactical Sentries (ANTS) Program (Contract #F04701-97-C-0016) funded by DARPA TTO (Dr. Ed Carapezza), Raytheon has also demonstrated a prototype snapshot mode, low cost, low power 15x31 Micro Infrared Camera (MIRC) for unattended ground sensor applications. In addition, the 15x31 array is also slated for production for use in industrial process monitoring and diagnostics applications. Under the ANTS program, the 15x31 array is presently being upgraded to a 120x160 array for improved resolution and field-of-view.

the proposed Phase II will be carried out in five Tasks:

Task I. Define Integrated Package Design(AFR and Raytheon). To determine the design parameters for an integrated etalon/bolometer/readout package suitable for 1D or 2D spectroscopic applications.

Task II. Fabricate Microbolometer Array (Raytheon) - To fabricate and test amorphous silicon microbolometer arrays with integrated readout electronics for integration with etalon array.

Task III. Design and Fabricate GIF Etalon Array (AFR) - To design and fabricate the GIF etalon array for integration with microbolometer arrays.

Task IV. Assemble and Test Integrated Package and Spectrometer Systems. (AFR). Assemble spectrometer systems with GIF/Bolometer arrays and associated optics.

Task V. Test and Evaluate System - AF13R will perform detailed infrared/spectroscopy characterization tests. Using several IR applications, demonstrate the sensitivity and resolution of the spectrometer. Compare spectrometer with competing technologies with regard to cost and range of application.

6.0 PERSONNEL SUPPORTED

Personnel Supported or associated with this program:

Dr. David G. Hamblen - PI, AFR

Dr. Thomas Schimert - Raytheon/TI Systems

Mr. Ka Wa Chu - Technical Staff AFR, cooperative student from Cornell University.

Ms. Marie DiTaranto - Technical Staff AFR

Mr. Robert M. Carangelo – Consultant and co-inventor of the GIF design.

REFERENCES

1. U.S. Dept. of Energy, SBIR program (DE-FG05-93ER81507).
2. T. Schimert, R. Gooch, W. McCardel, R. Terrill, S. Borrello, J. Whitney, P. Kroger, and A.Ahne, "Low Cost Uncooled a-Si Microbolometer -based Infrared Environmental Gas Sensor Technology". presented at the *1996 AWMA International Symposium on Optical Sensing for Environmental and Process Monitoring*", 6-8 November, 1996, Dallas Texas (to be published in the conference proceedings).
3. T. Schimert, R. Gooch, R. Keller, W. McCardel, B. Ritchey, R. Terrill, S. Borrello, "Design Considerations for Enhanced Performance and Frequency Response in Low Cost Uncooled a-Si Microbolometer Arrays". to appear in the *Proceedings for the 1997 Meeting of the IRIS Specialty Group on Materials and Infrared Detectors*, 28-31 July 1997, Monterey, CA.
4. D.B. Fenner and R.M. Carangelo, U.S. Patent # 5,354,989 (Oct 1994).
5. Baum, T., Schiffrin, D. J., "AFM study of Surface Finish Improvement by Ultrasound in the Anisotropic Etching of Si<100> in KOH for Micromachining Applications", J.Micromech. Microeng. 7 (1997) 338-342.
6. D.B. Fenner, R.M. Carangelo, D.G. Hamblen, P.-J. Kung, and J.I. Budnick, "Infrared Bolometer and Silicon-Etalon Arrays For Transform Spectrometer On-A-Chip", *Euro. Conf. Appl. Supercon.*, Edinburgh, Scotland, July 1995, *Inst. Phys. Conf. Series,* No. 148, Vol. 2, pp. 1231-1234 (1995).
7. D.B. Fenner, Qi Li, W.D. Hamblen, M.E. Johansson, D.G. Hamblen, L. Lynds, and J.I. Budnick, "Optical and Thermal Performance Advantages for Silicon Substrates in YBCO Bolometer Devices", *IEEE Transactions on Applied Superconductivity* **3**, 2104-2106 (1993).
8. Q. Li, D.B. Fenner, W.D. Hamblen, and D.G. Hamblen, "Epitaxial YBaCuO Bolometers On Micromachined Windows In Silicon Wafers", *Appl. Phys. Lett.* **62**, 2428-2430 (1993).
9. H. Van de Stadt and J.M. Muller, "Multimirror Fabry-Perot Interferometers", *Opt. Soc. Am.* **A2**, 1363-1370 (1985).
10. P.B. Hays and H.E. Snell, "Multiplex Fabry-Perot Interferometer", *Appl. Opt.* **30**, 3108-3113 (1991).
11. J. Farhoomand and R. E. McMurray,Jr., NASA APL 58, 622 (Feb 1991).
12. D.B. Fenner and R.M. Carangelo, U.S. Patent # 5,354,989 (Oct 1994).

Appendix A: Figures

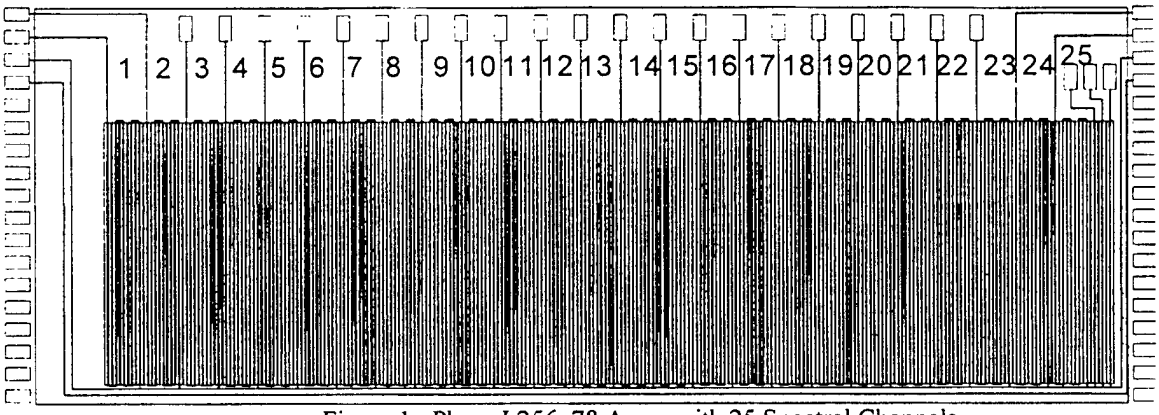

Figure 1. Phase I 256x78 Array with 25 Spectral Channels
Using Direct Address Bondpad per Channel.

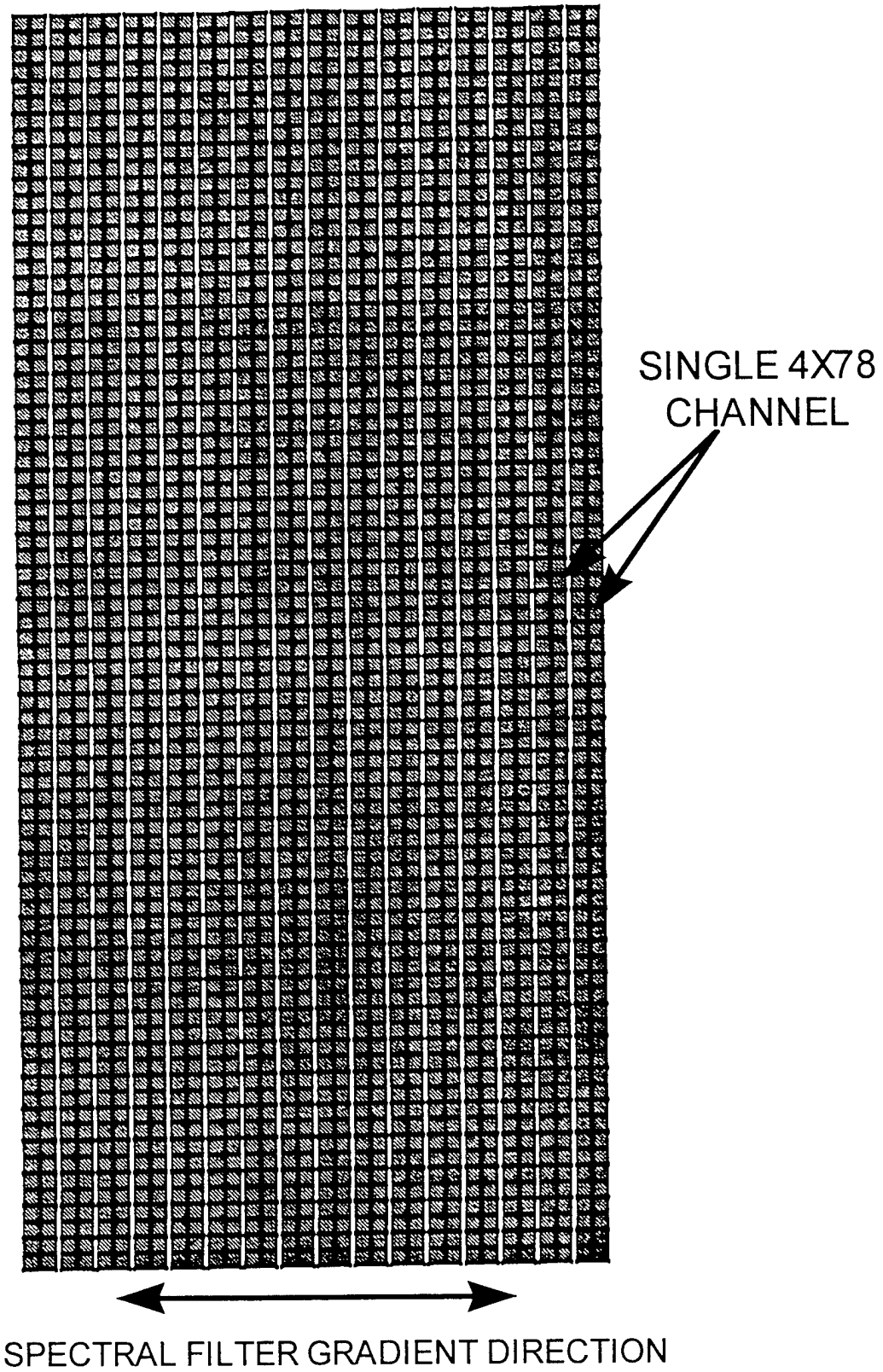

Figure 2. 16 Columns of the 64 channel Microbolometer Array Layout.

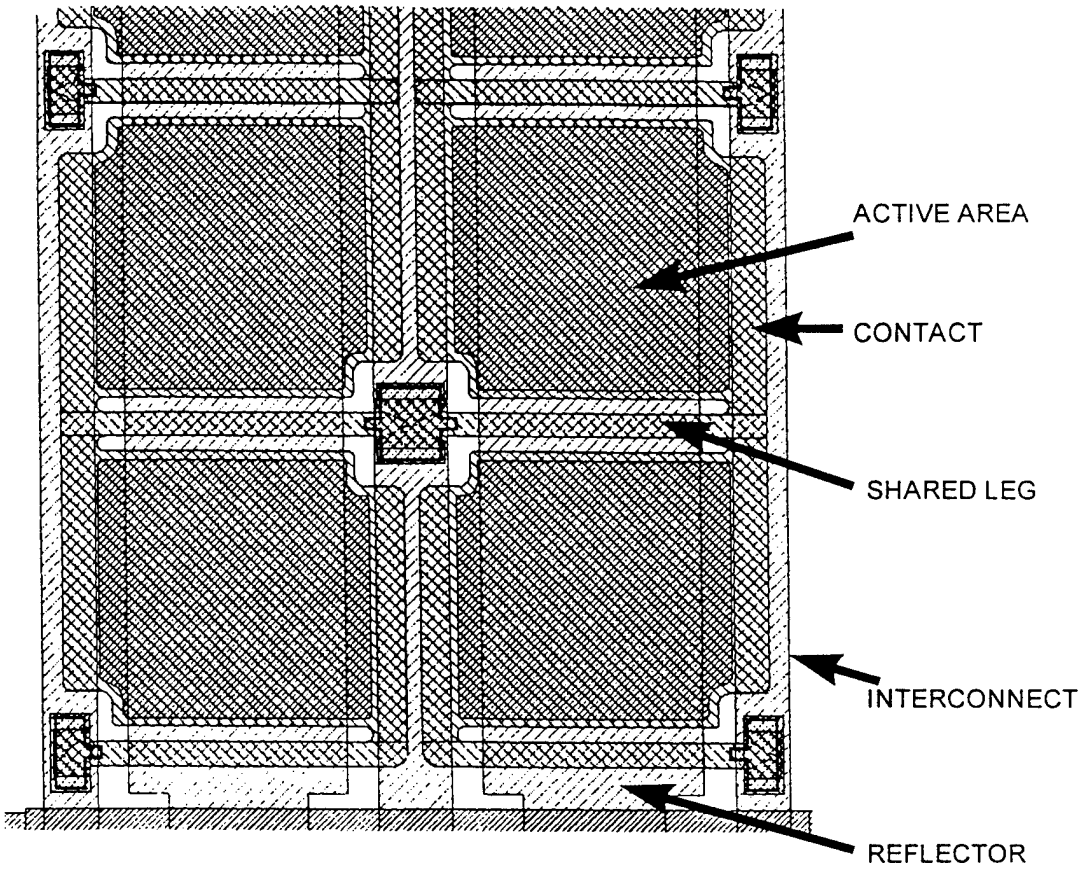

Figure 3. Detailed view of 4 pixel elements of a single superpixel array.

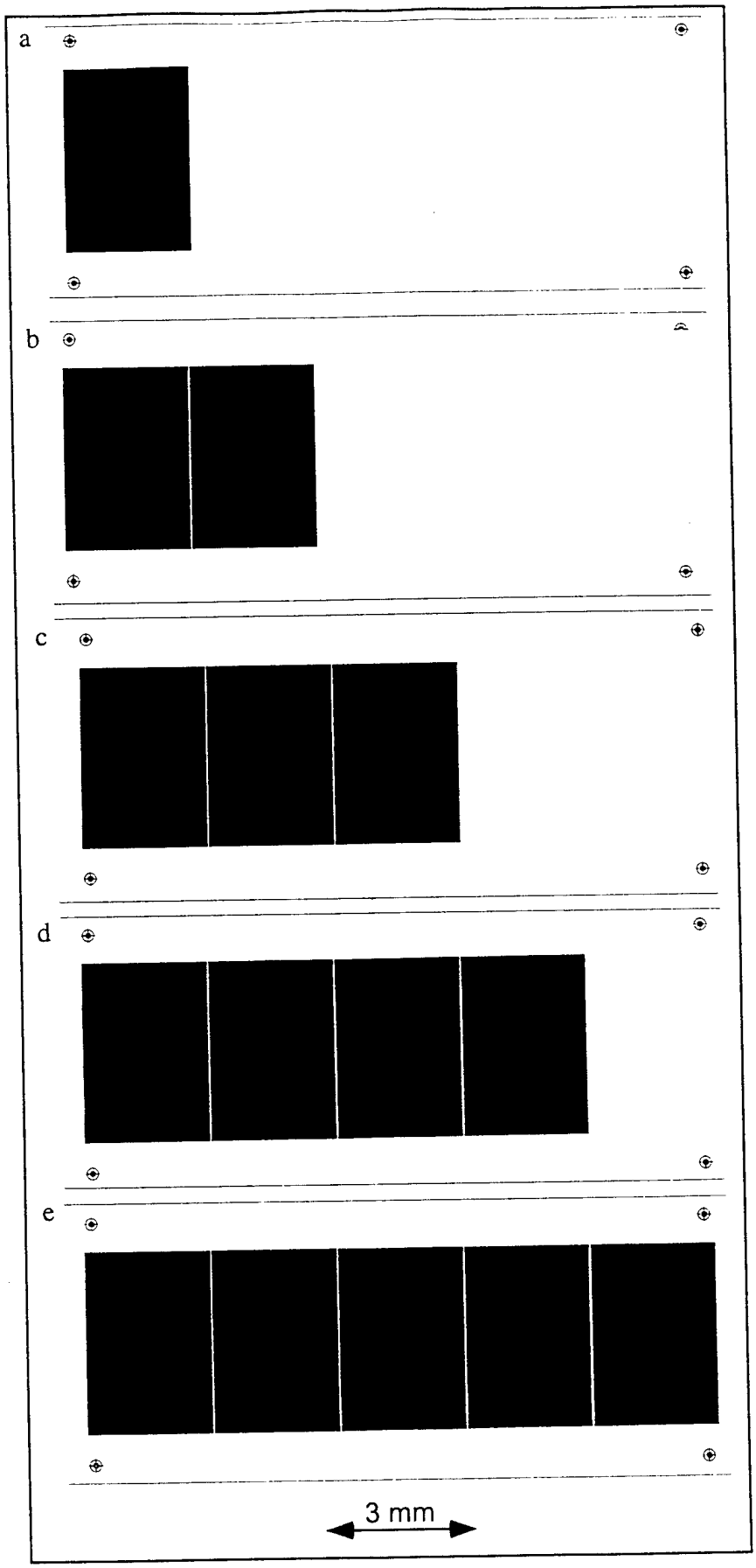

Figure 4. Layout of the Paper Masks for the 1x5 Etalon Array, showing the 5 separate masks used.

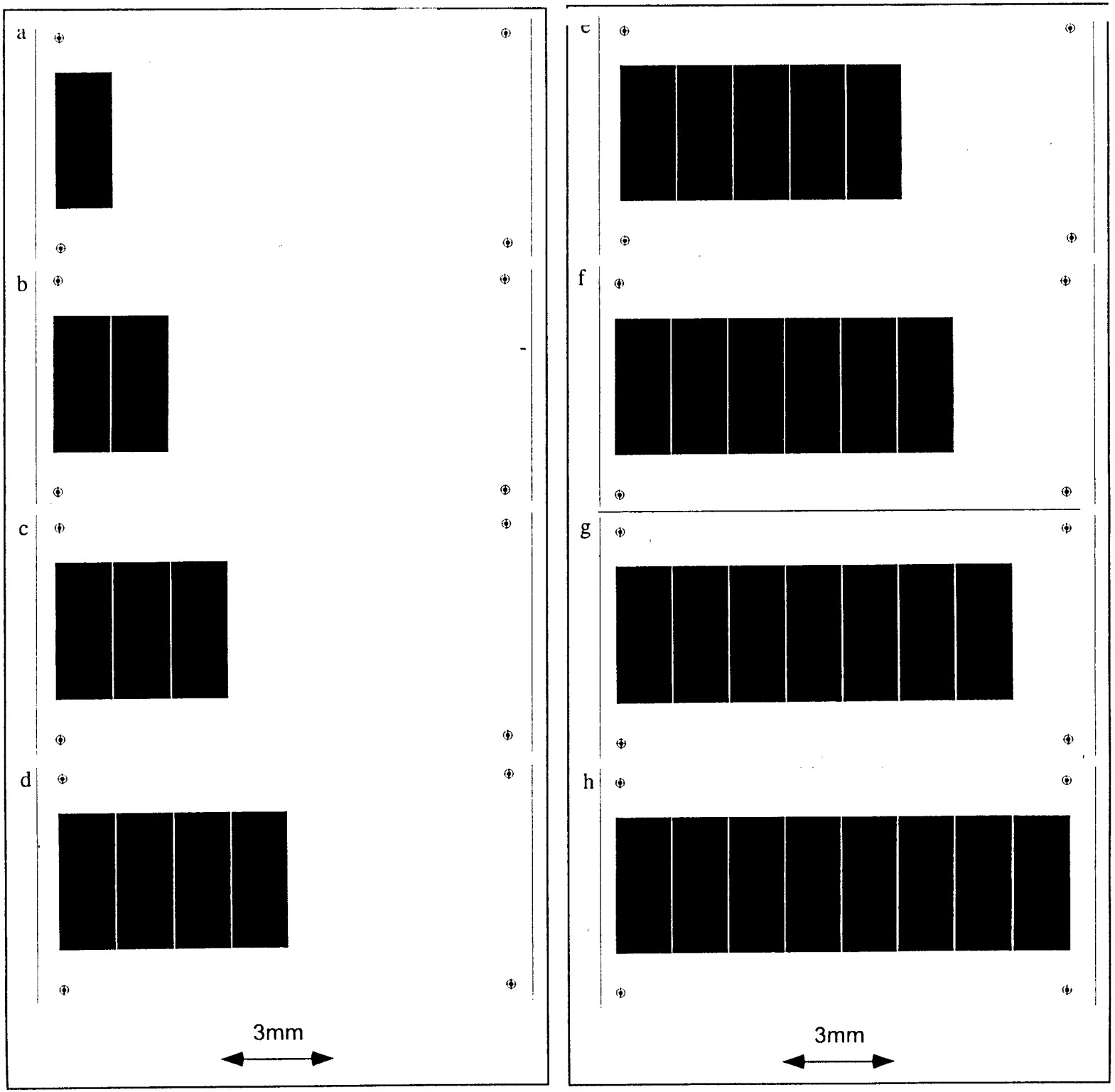

Figure 5. Layout of the Paper Masks for the 1x8 Etalon Array, showing the 8 separate masks used.

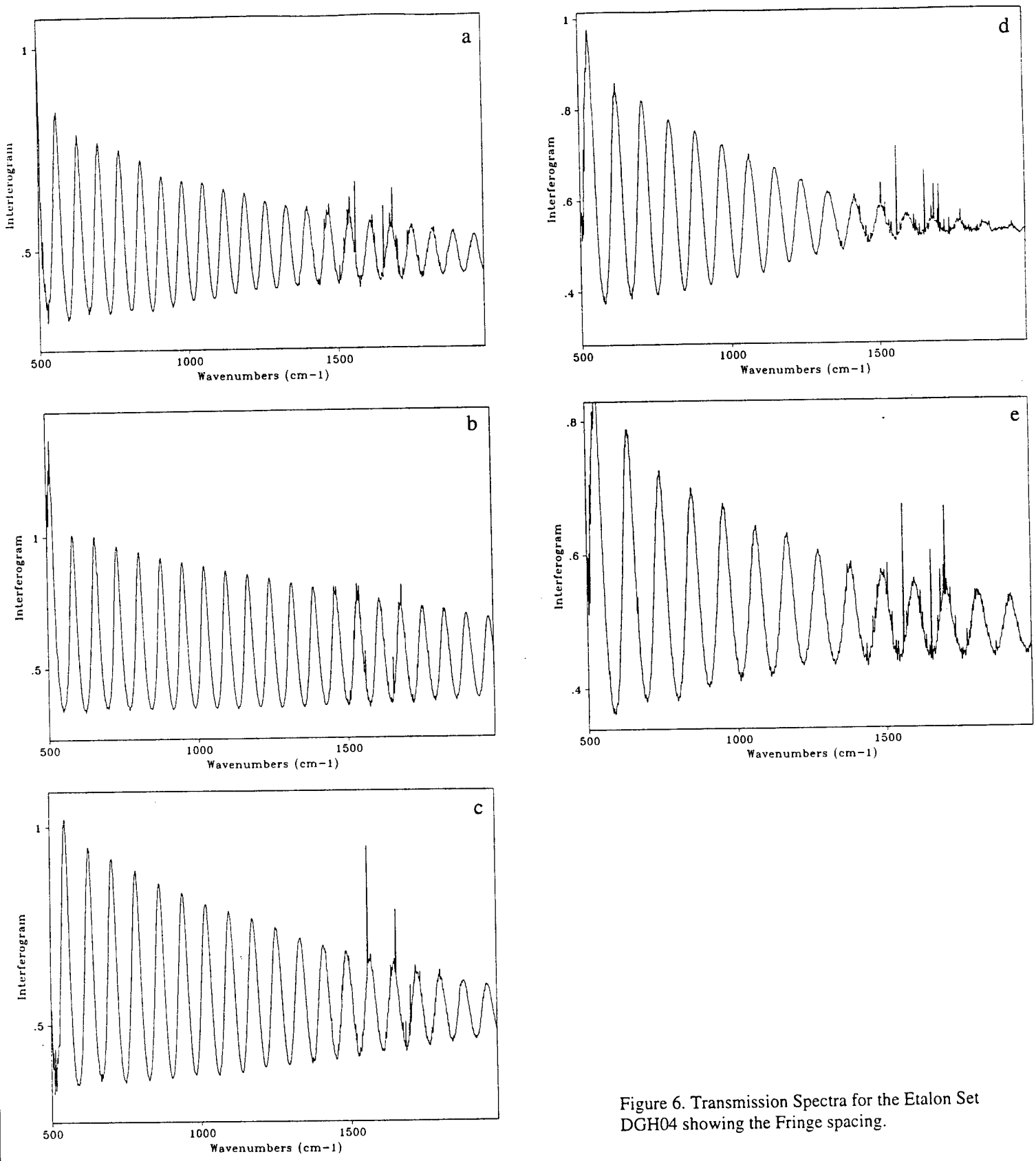

Figure 6. Transmission Spectra for the Etalon Set DGH04 showing the Fringe spacing.

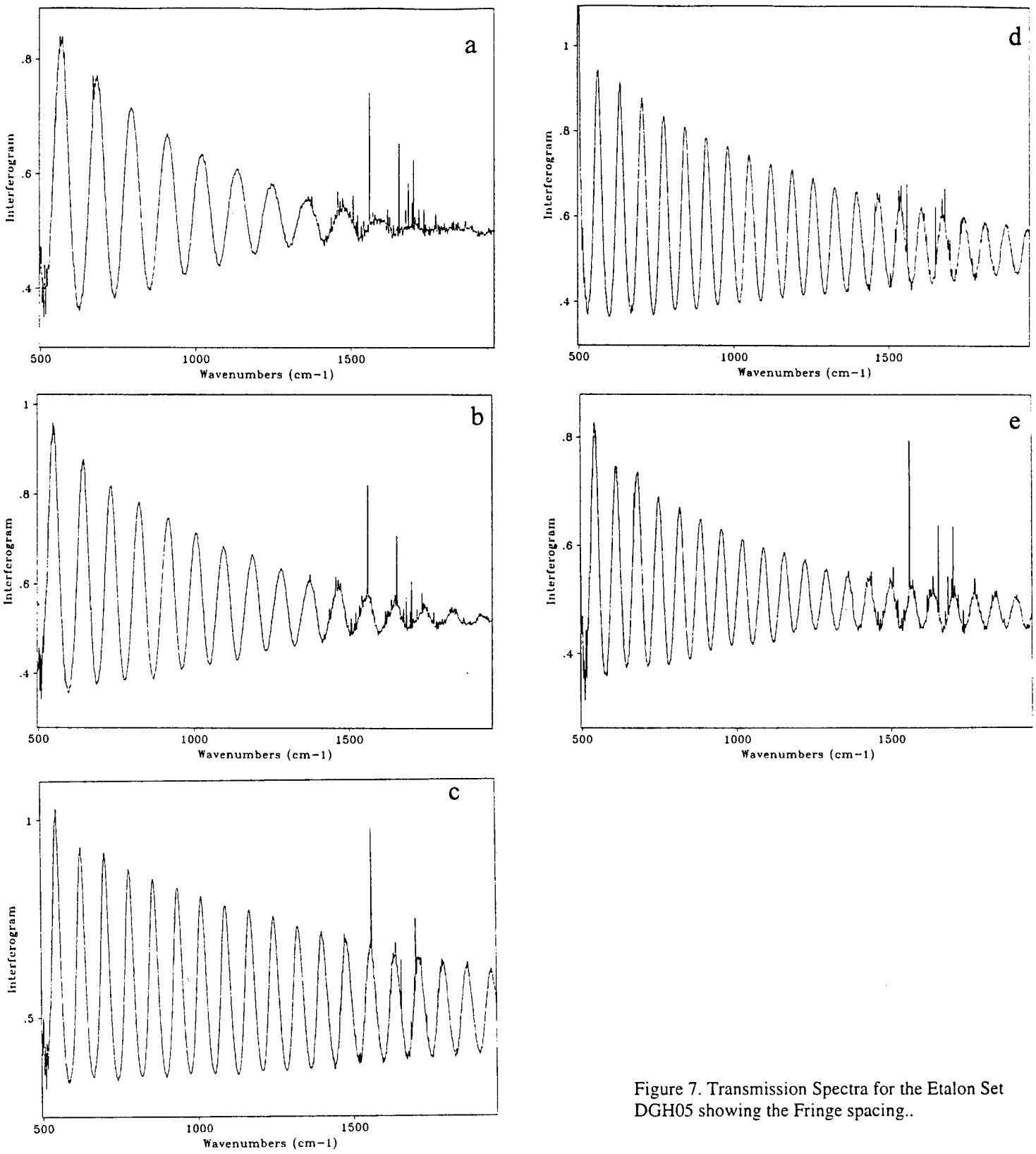

Figure 7. Transmission Spectra for the Etalon Set DGH05 showing the Fringe spacing..

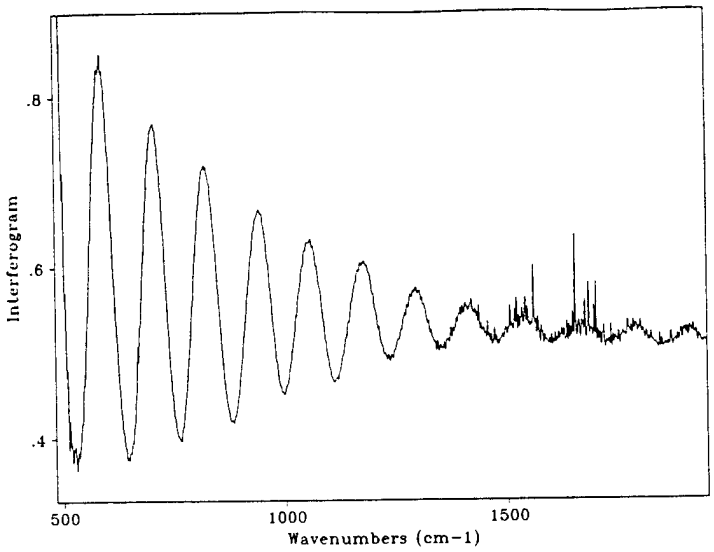

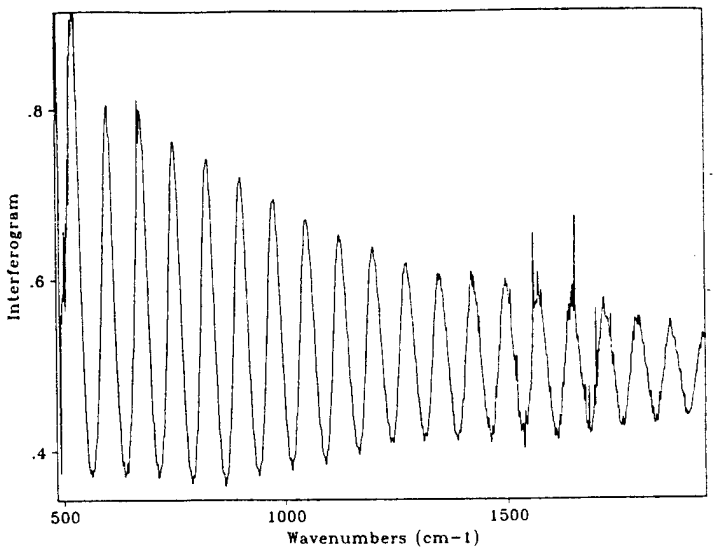

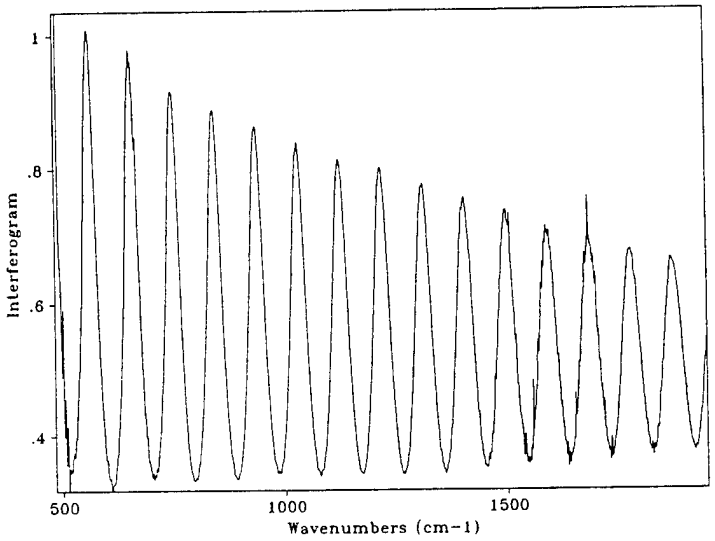

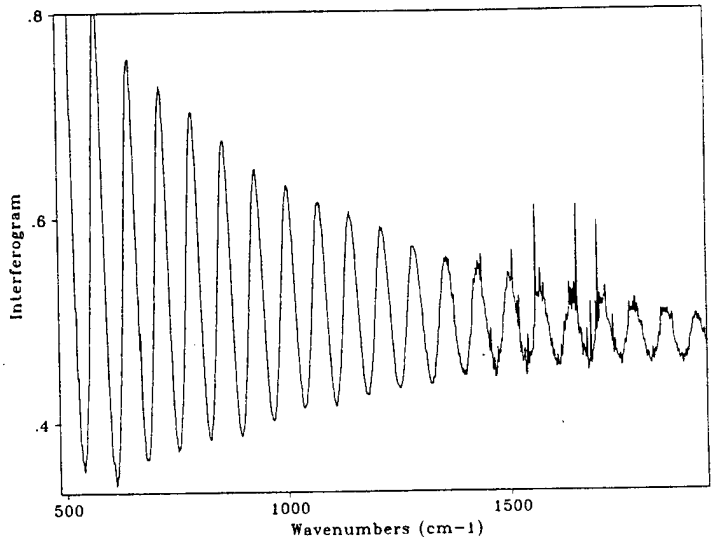

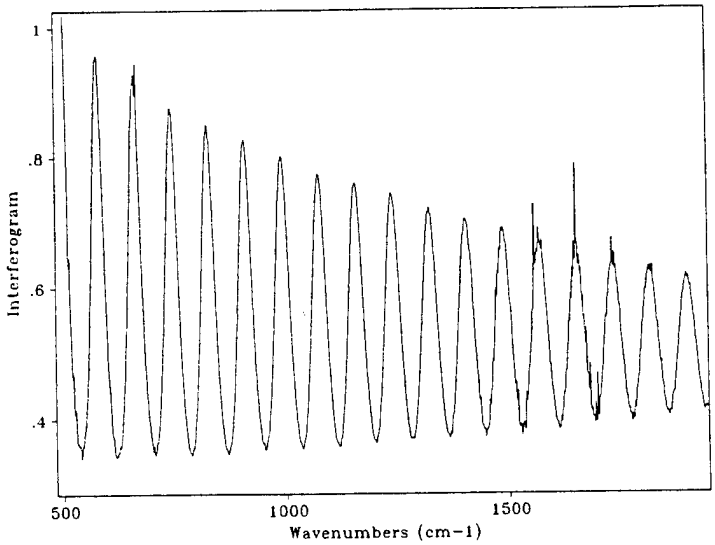

Figure 8. Transmission Spectra for the Etalon Set DGH06 showing the Fringe spacing.

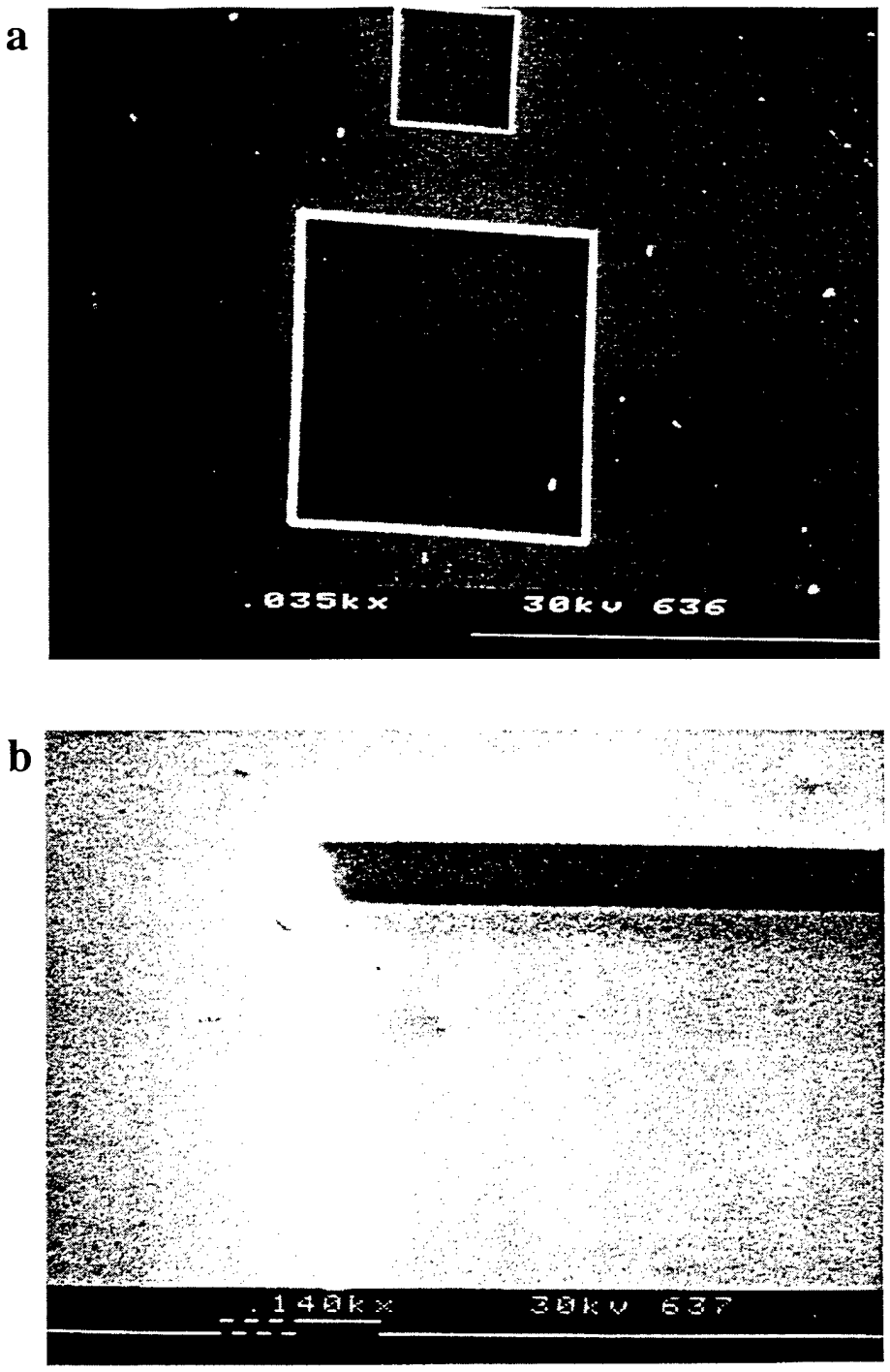

Figure 9. Photomicrograph of Holes Etched Using the Revise, Inc. Process.

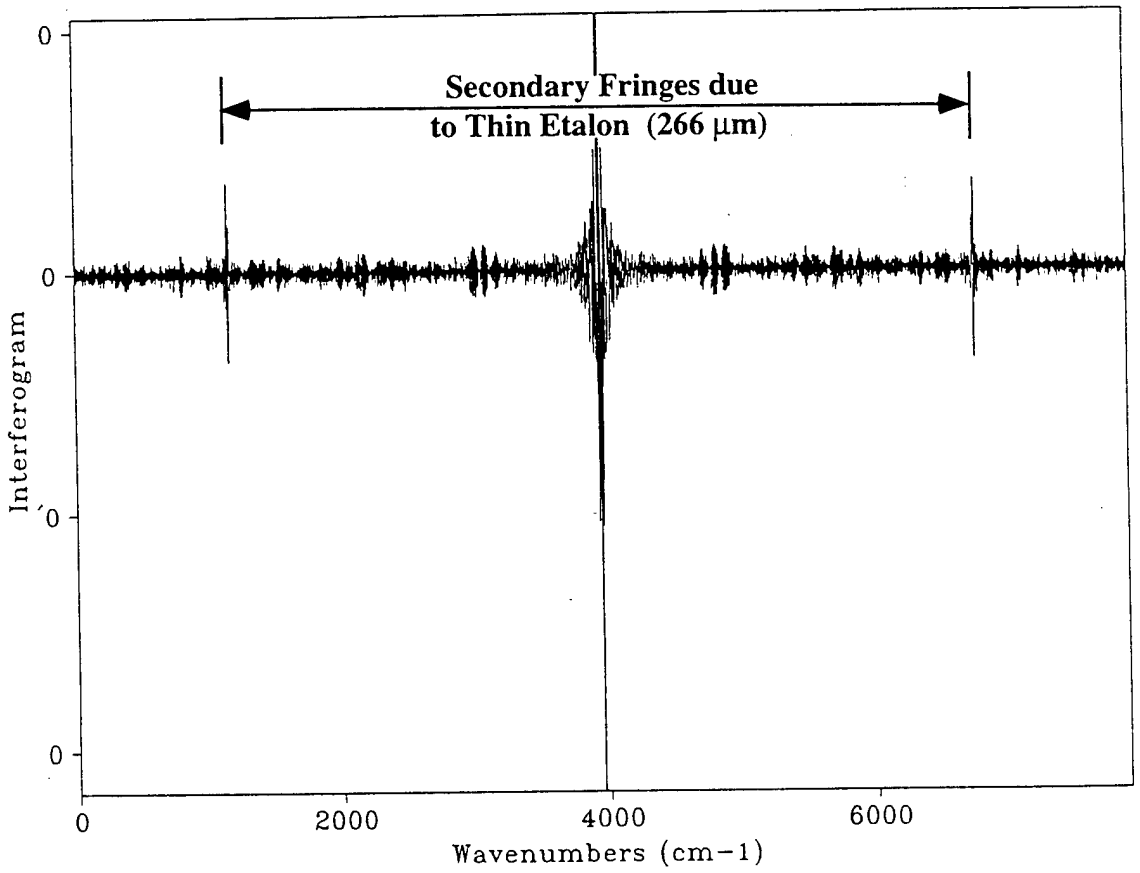

Figure 10. Transmission Spectrum of the Etalon Etched with the Revise, Inc. Process.

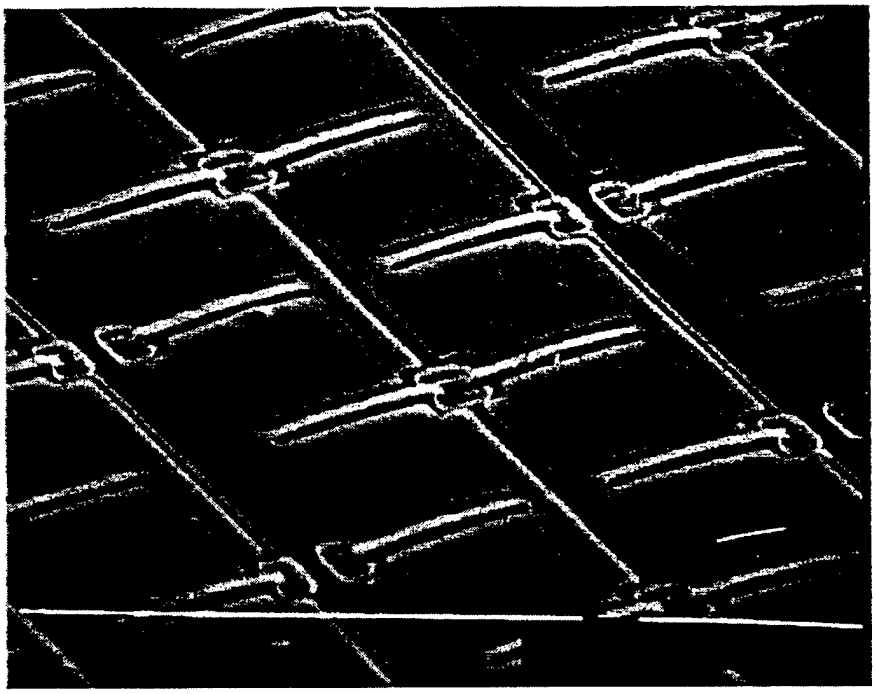

Figure 11. a-Si Suspended Membrane 50 μm Microbolometer Pixel Elements.

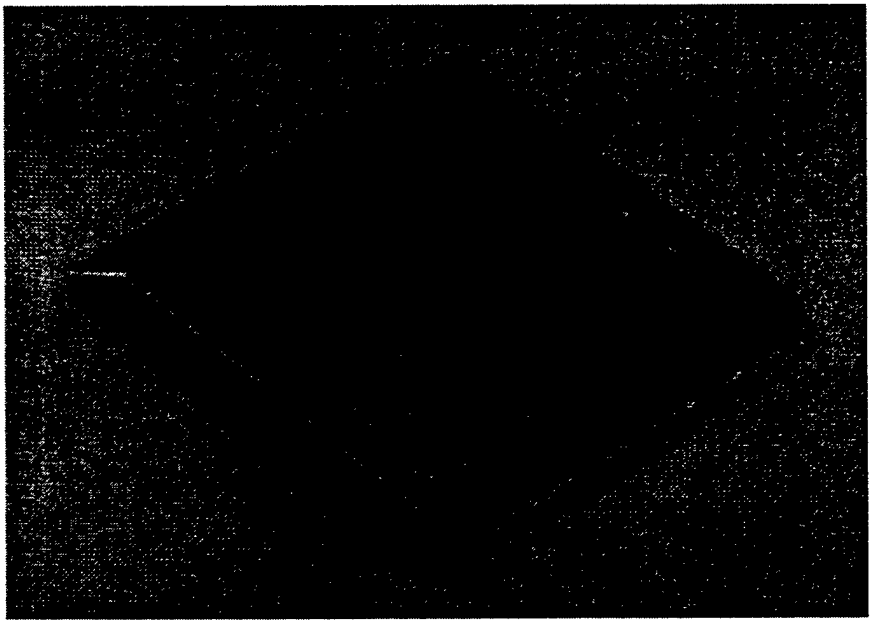

Figure 12. 84 pin Large area Ceramic Vacuum Package
with IR Transparent AR-coated Ge Lid.

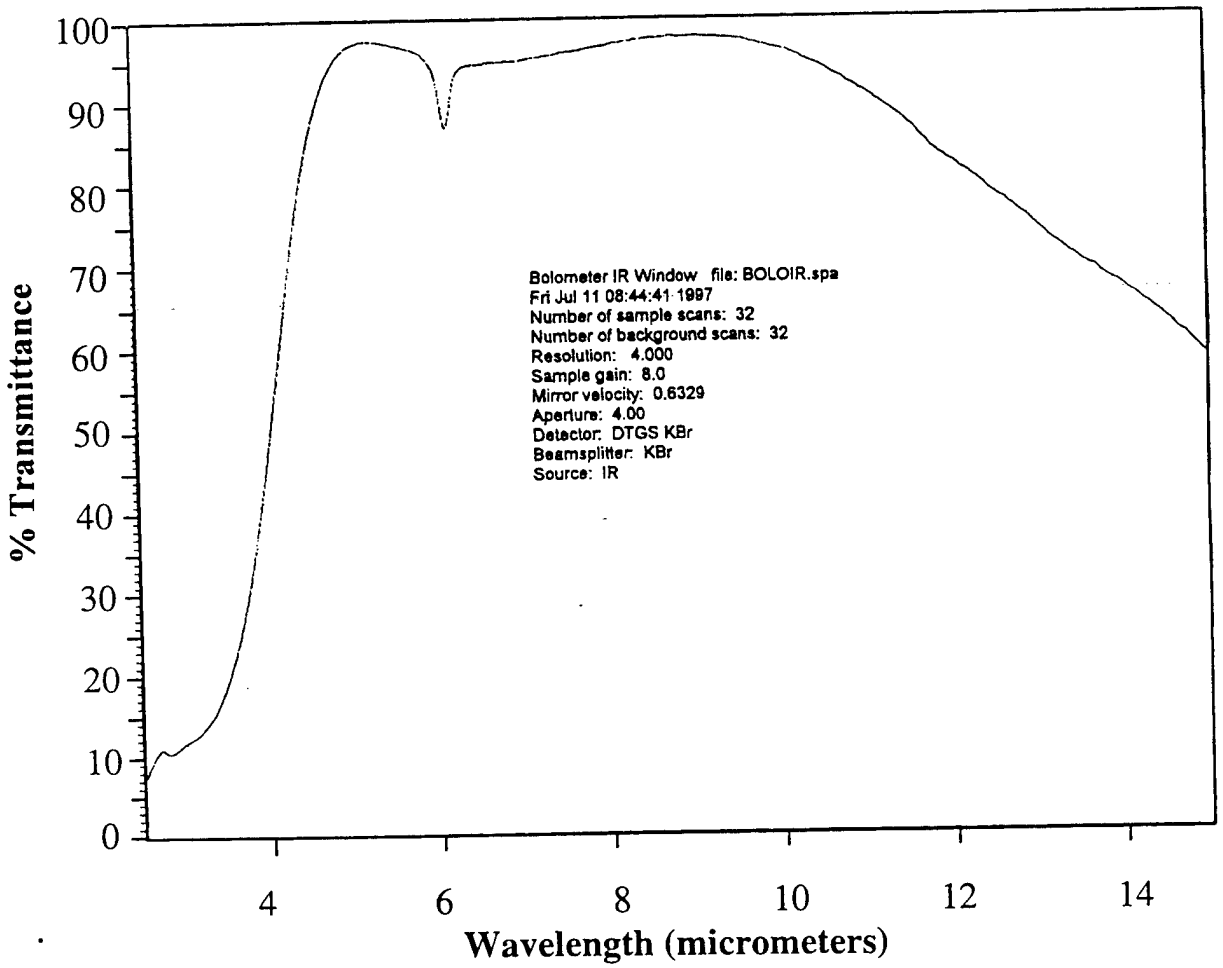

Figure 13. AR Coated Ge Lid Transmittance.

Transmission Examples

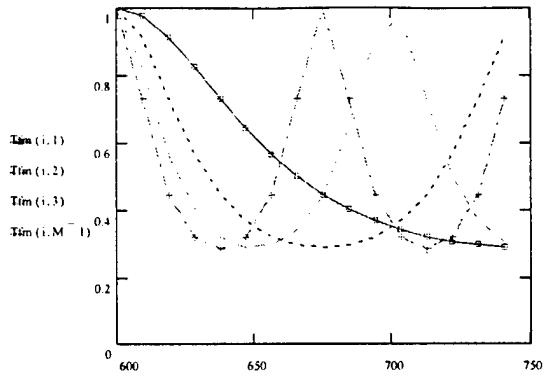

Figure 14. Transmission fringes for an array of four etalons showing the thinnest with one-half fringe through the thickest with 2 full fringes.

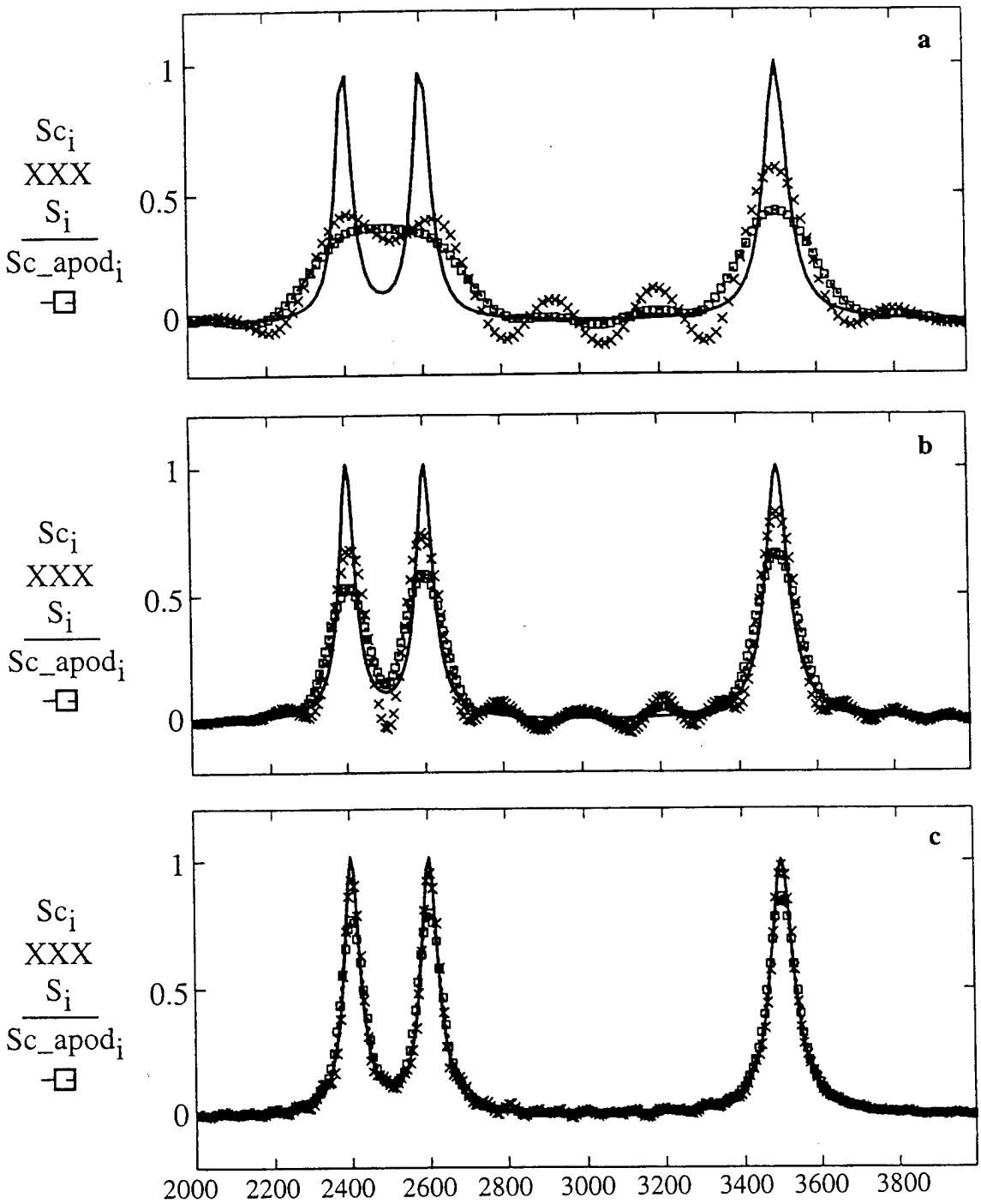

Figure 15. Simulated spectrum and transformed reconstruction of simulated spectrum for the frequency range 2000-4000 cm^{-1}, with a) 16 etalons, b) 32 etalons, and c) 64 etalons. The solid curve is the simulated spectrum, the x's are the reconstruction without apodization, and the boxes are with apodization.

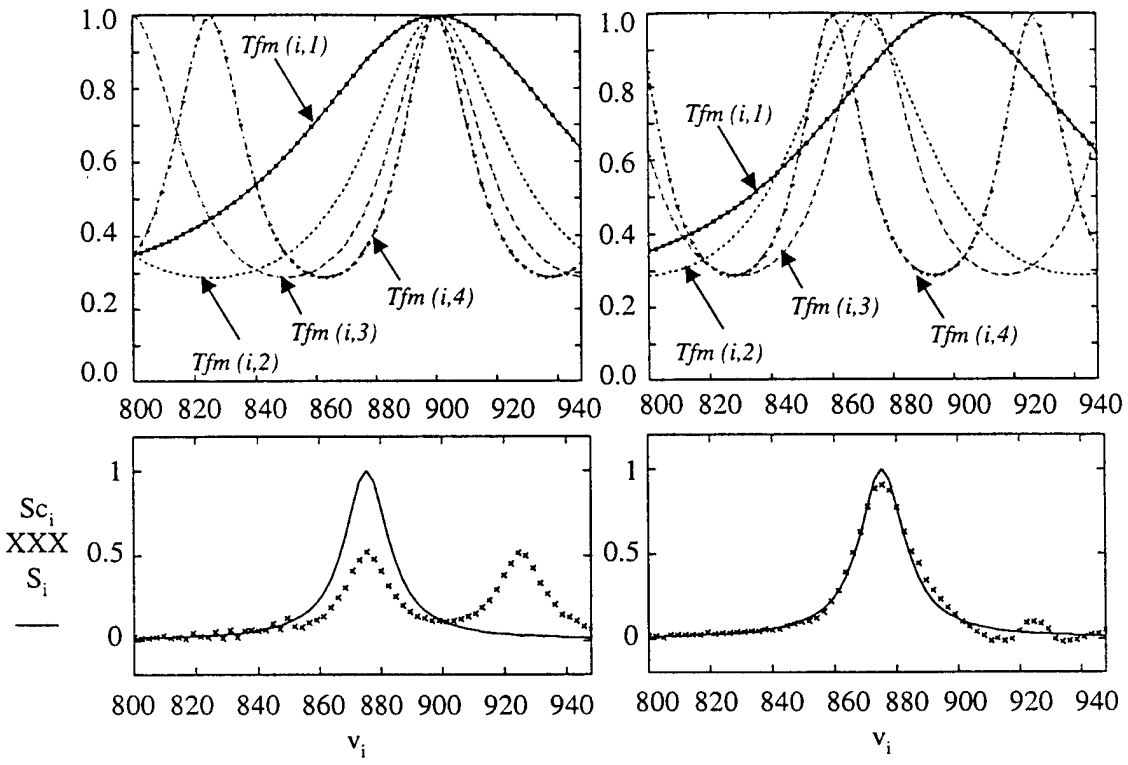

Figure 16. a) Transmission fringes for the same array as in Figure 1, but starting at 800 cm^{-1}; b) First four transmission fringes for set "Actual" in Table VI; c) Input and transform spectra for "Target" etalon set; and d) Input and transform spectrum for "Actual" etalon set.

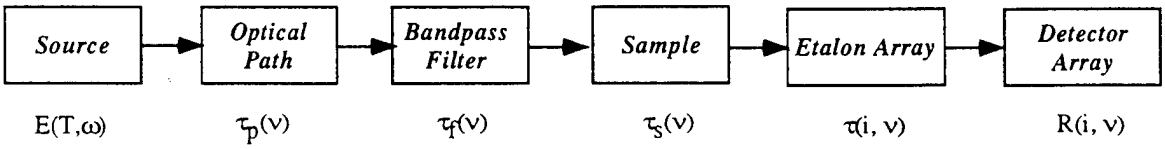

Figure17. Block Diagram of Spectrometer-on-a-Chip.

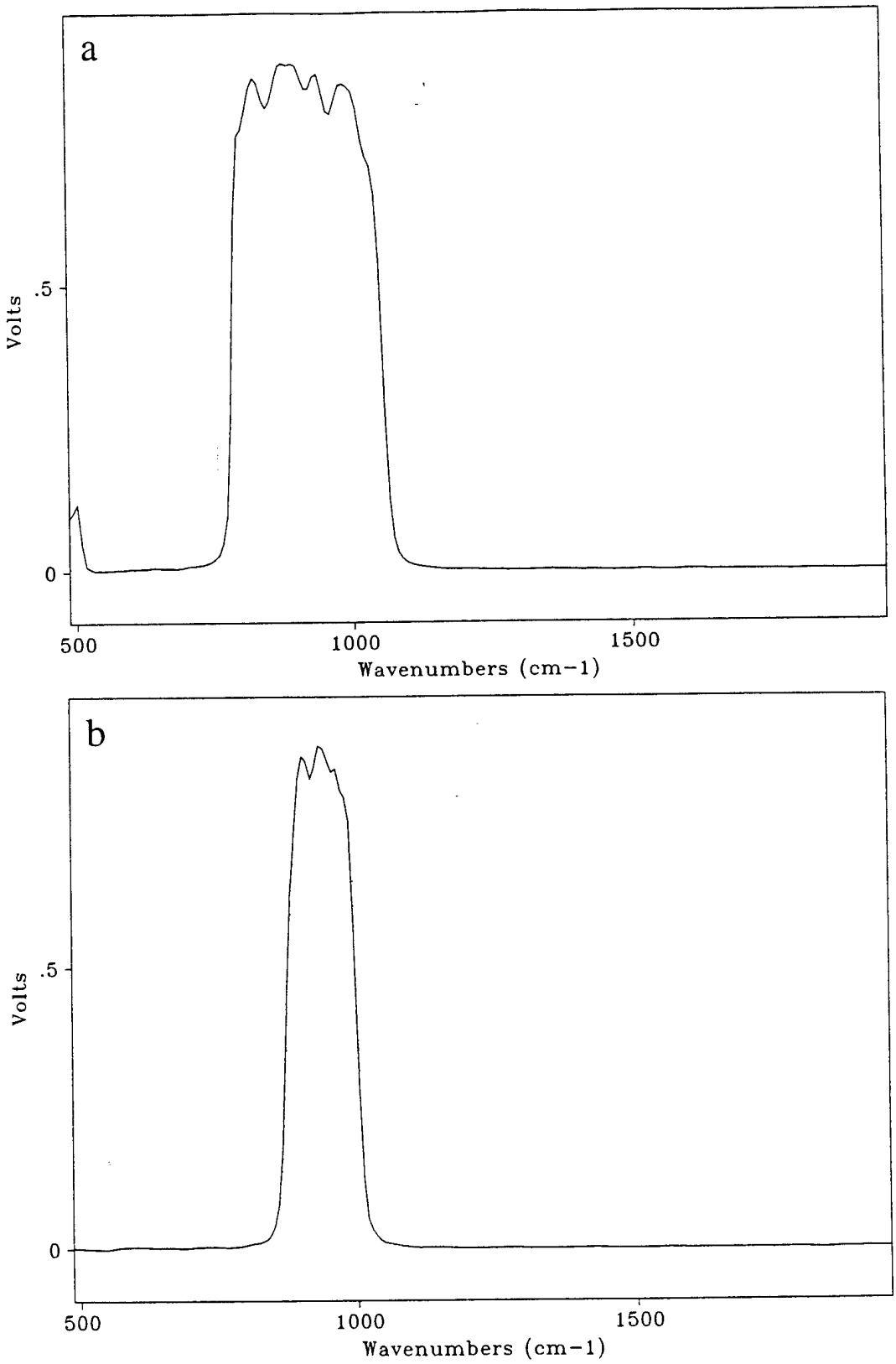

Figure 18. Transmission spectra for bandpass filters used.

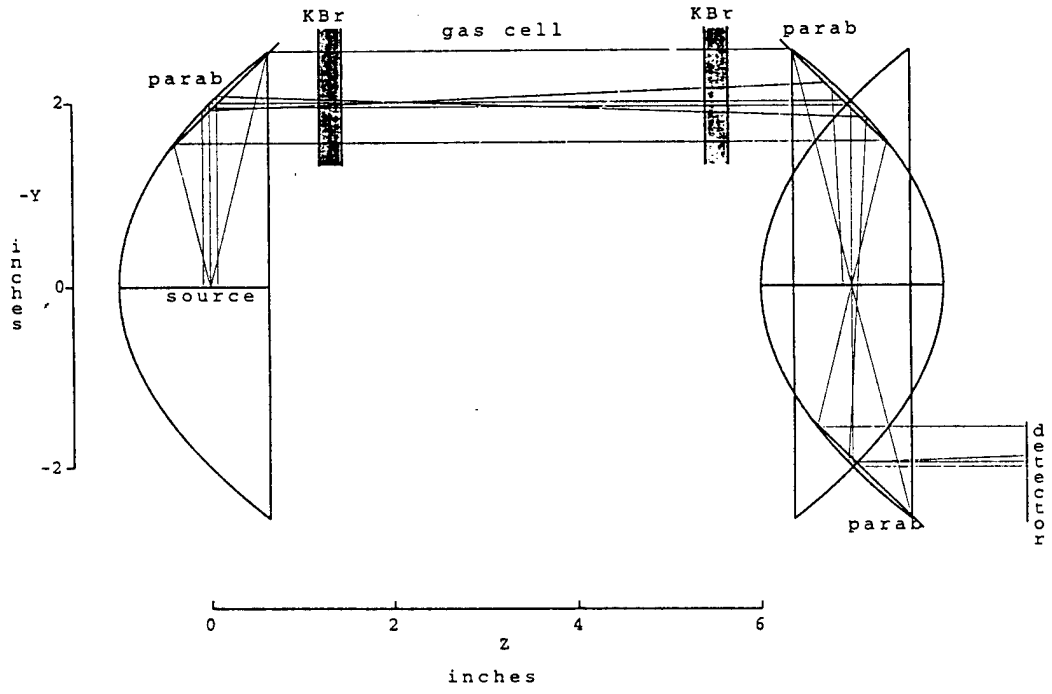

Figure 19. Top View of Optical Layout of Spectrometer for Ray Tracing Analysis.

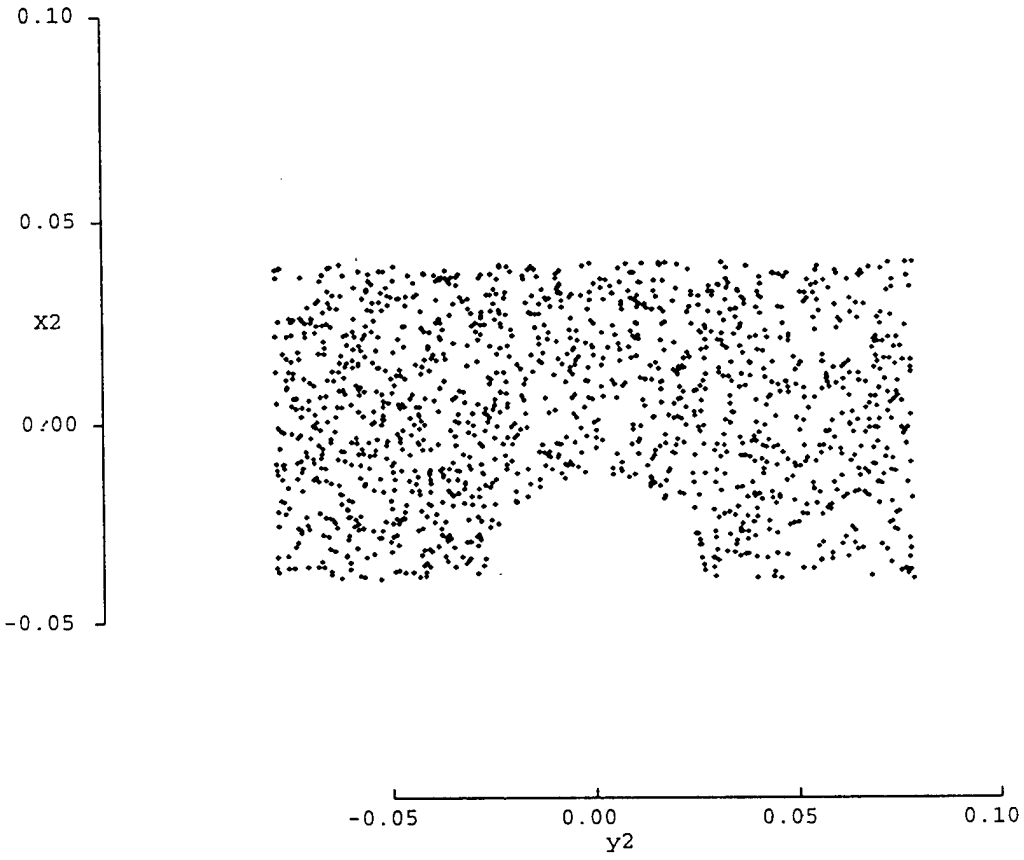

Figure 20. Ray Tracing analysis of Spectrometer- location of rays leaving the source.

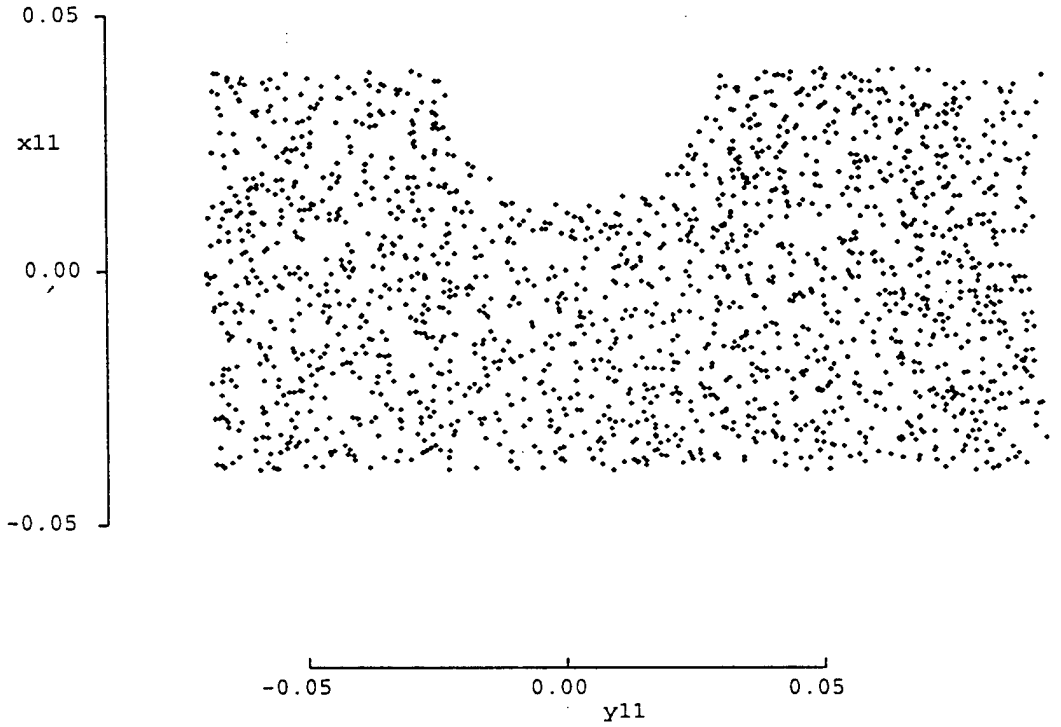

Figure 21. Ray Tracing Analysis of Spectrometer - location of rays passing through the center aperture (at the chopper).

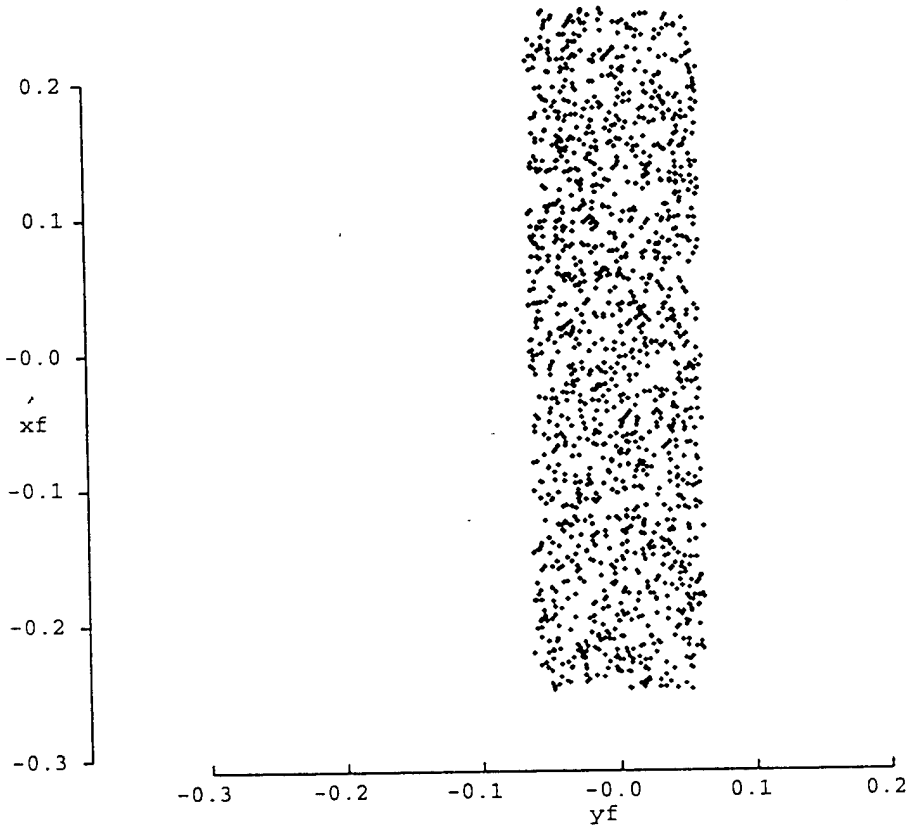

Figure 22. Ray Tracing Analysis of Spectrometer - location of rays arriving at detector.

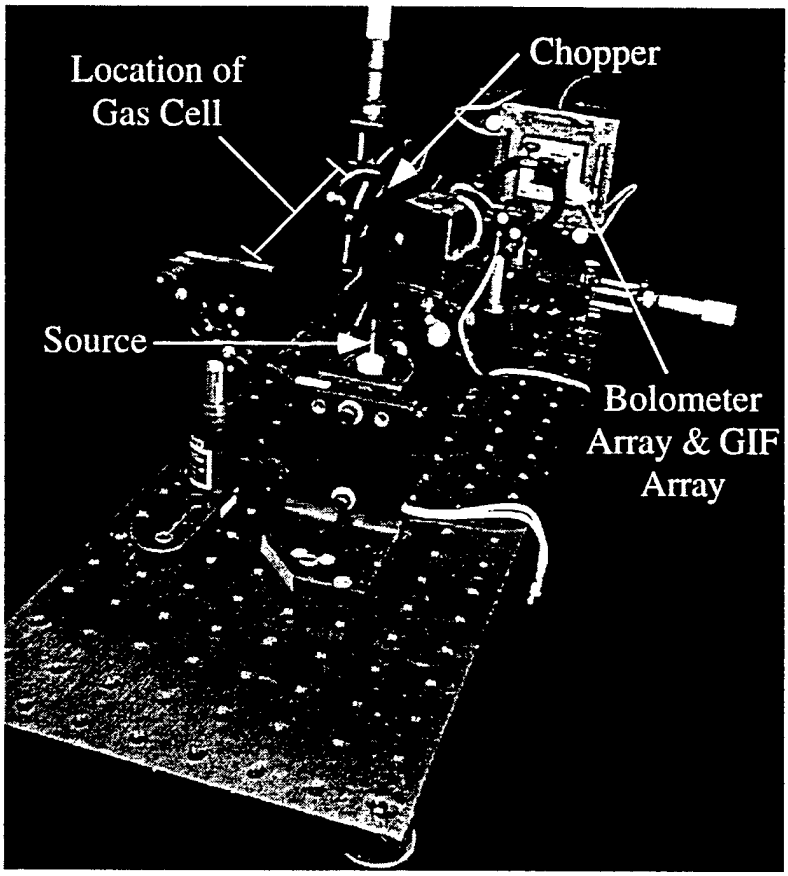

Figure 23. Photograph of Spectrometer.

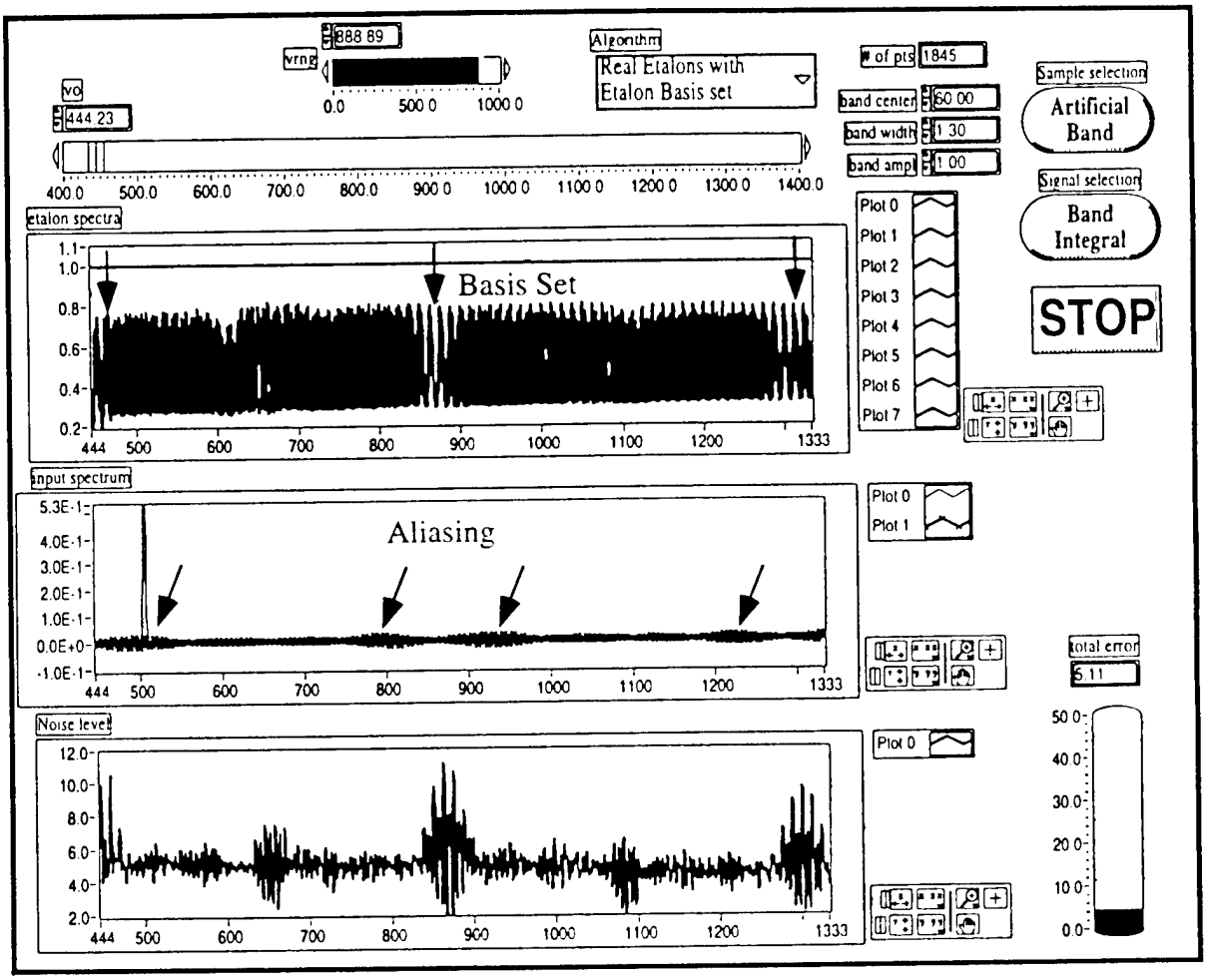

Figure 24. LabView Simulations of Etalon Set Containing only Thick Etalons. Determination of Effective Bandwidth.

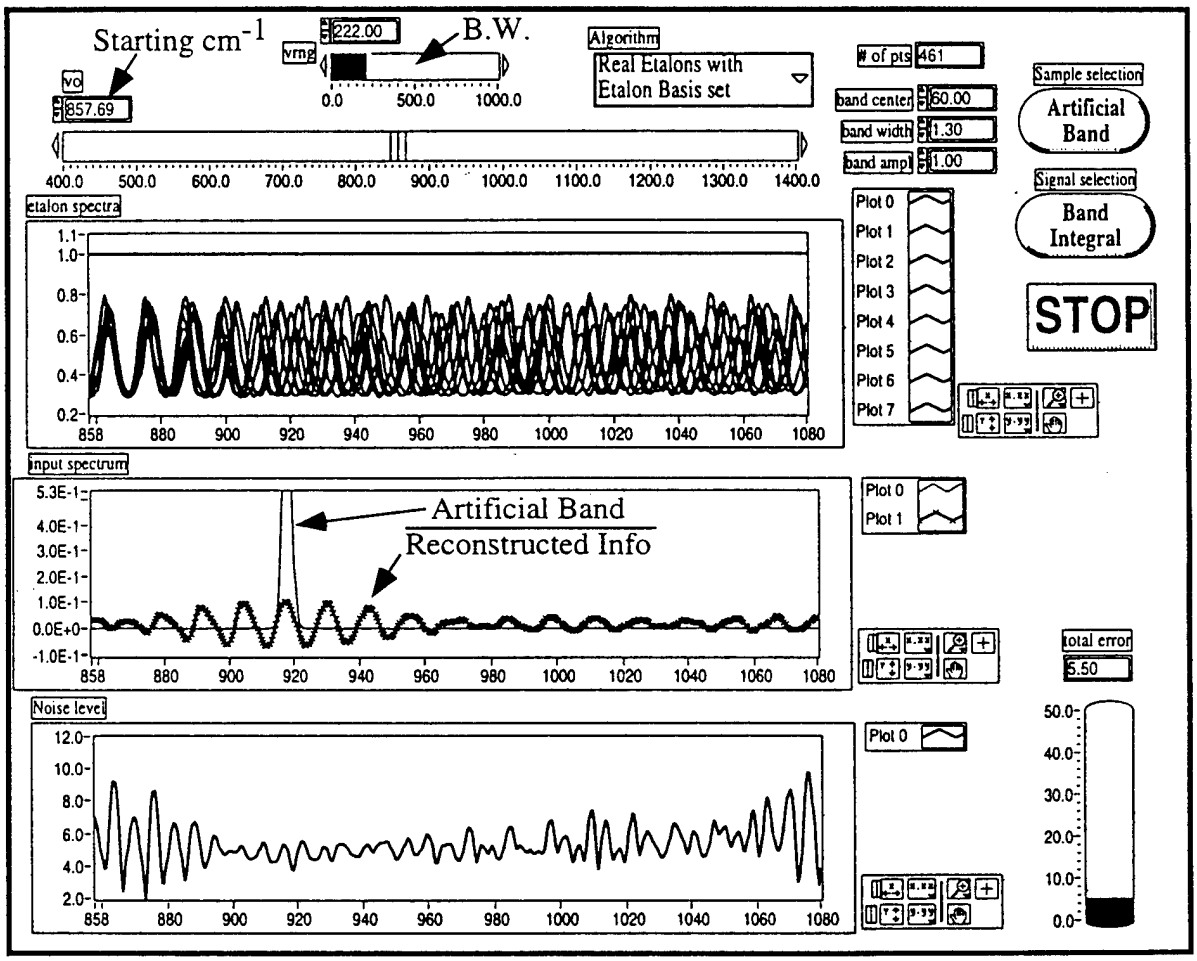

Graph A

Graph B

Graph C

Figure 25. LabView Simulations of Etalon Set Containing only Thick Etalons (set T6), showing that narrow features are detected, but not in detail.

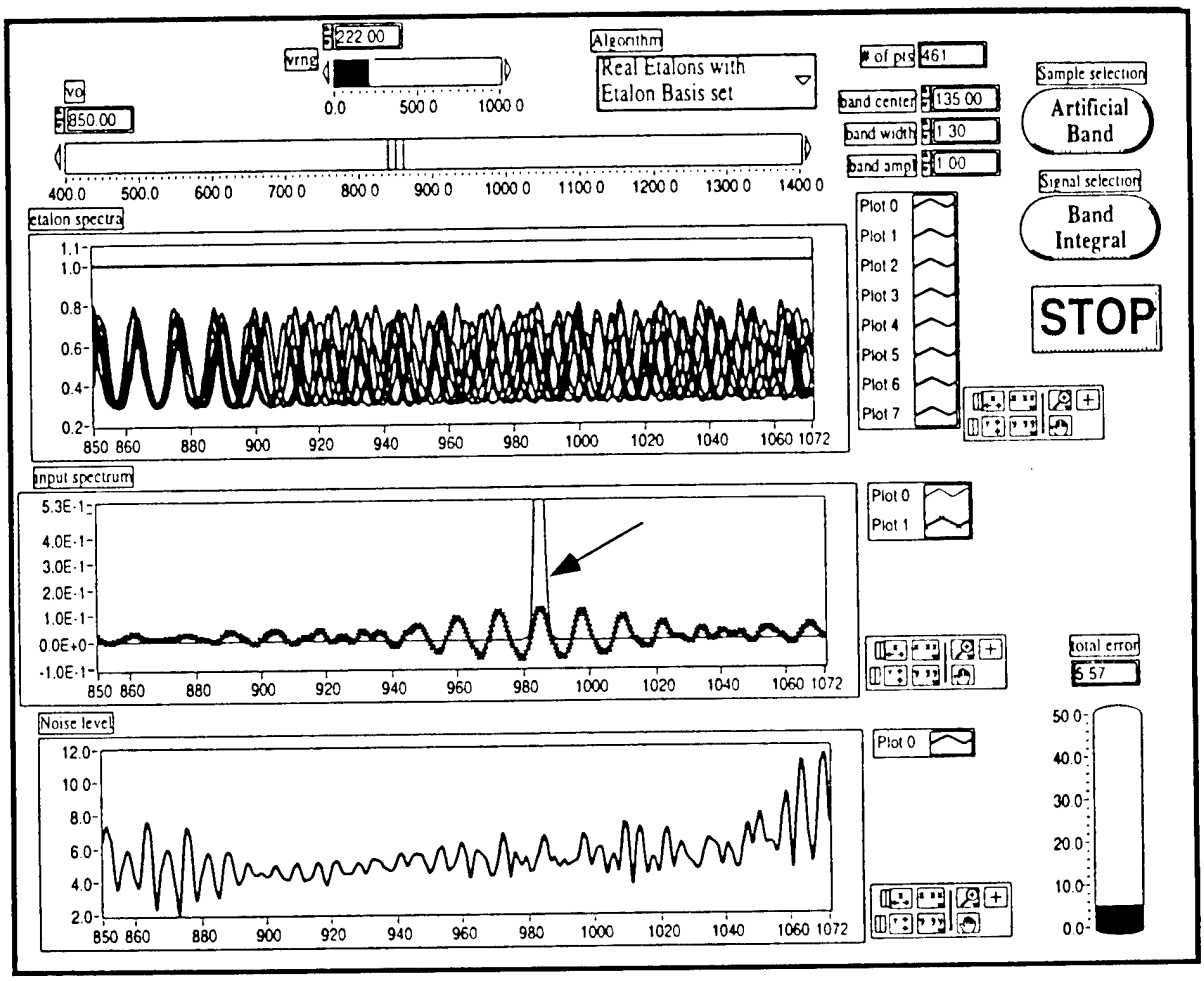

Figure 26. LabView Simulations of Etalon Set Containing only Thick Etalons, showing that narrow features are detected anywhere within the bandpass.

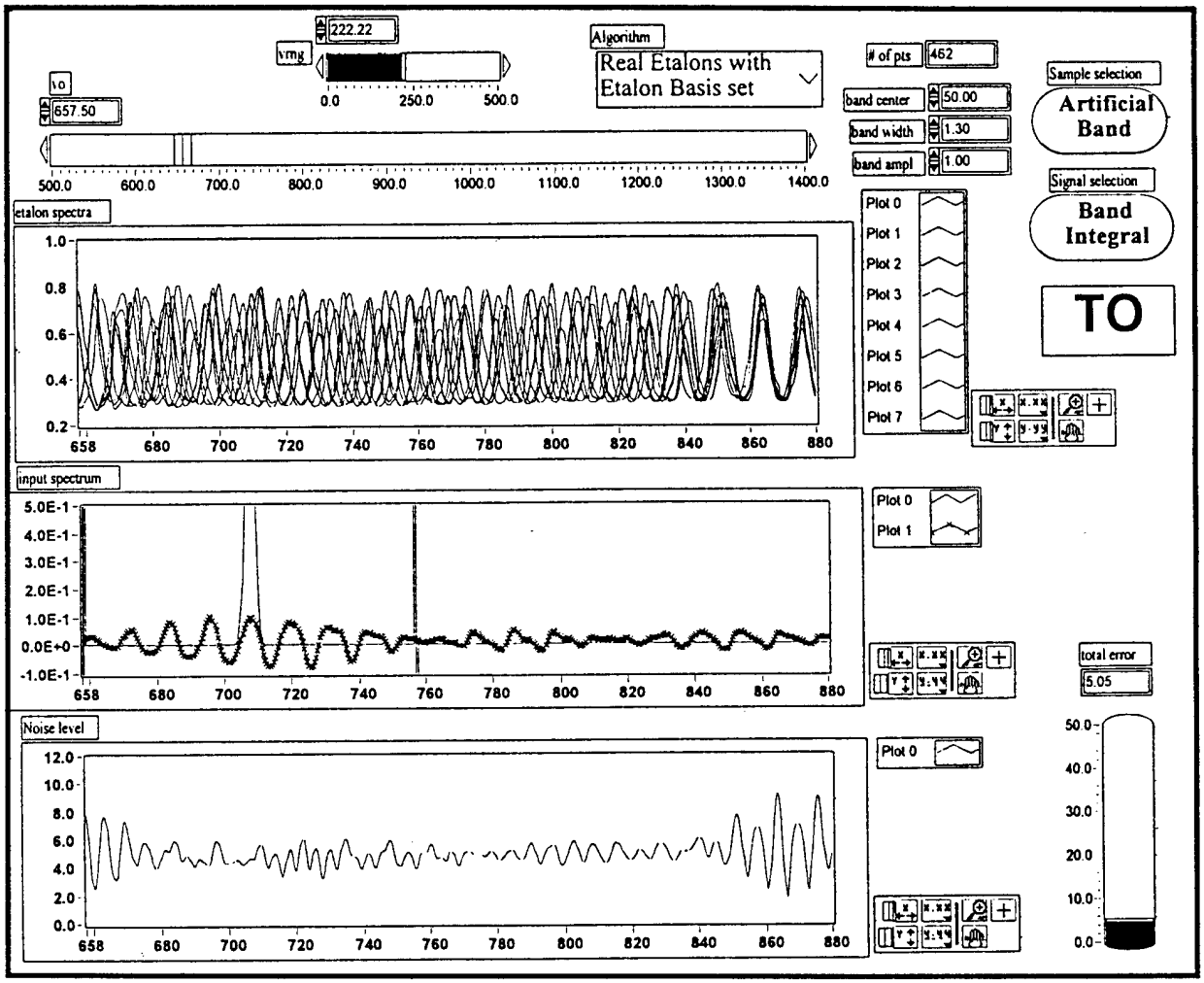

Figure 27. LabView Simulations of Etalon Set Containing only Thick Etalons, showing that narrow features are detected anywhere within the bandpass., and that the bandpass can be located in any valid Nyquist zone.

Graph A

Graph B

Graph C

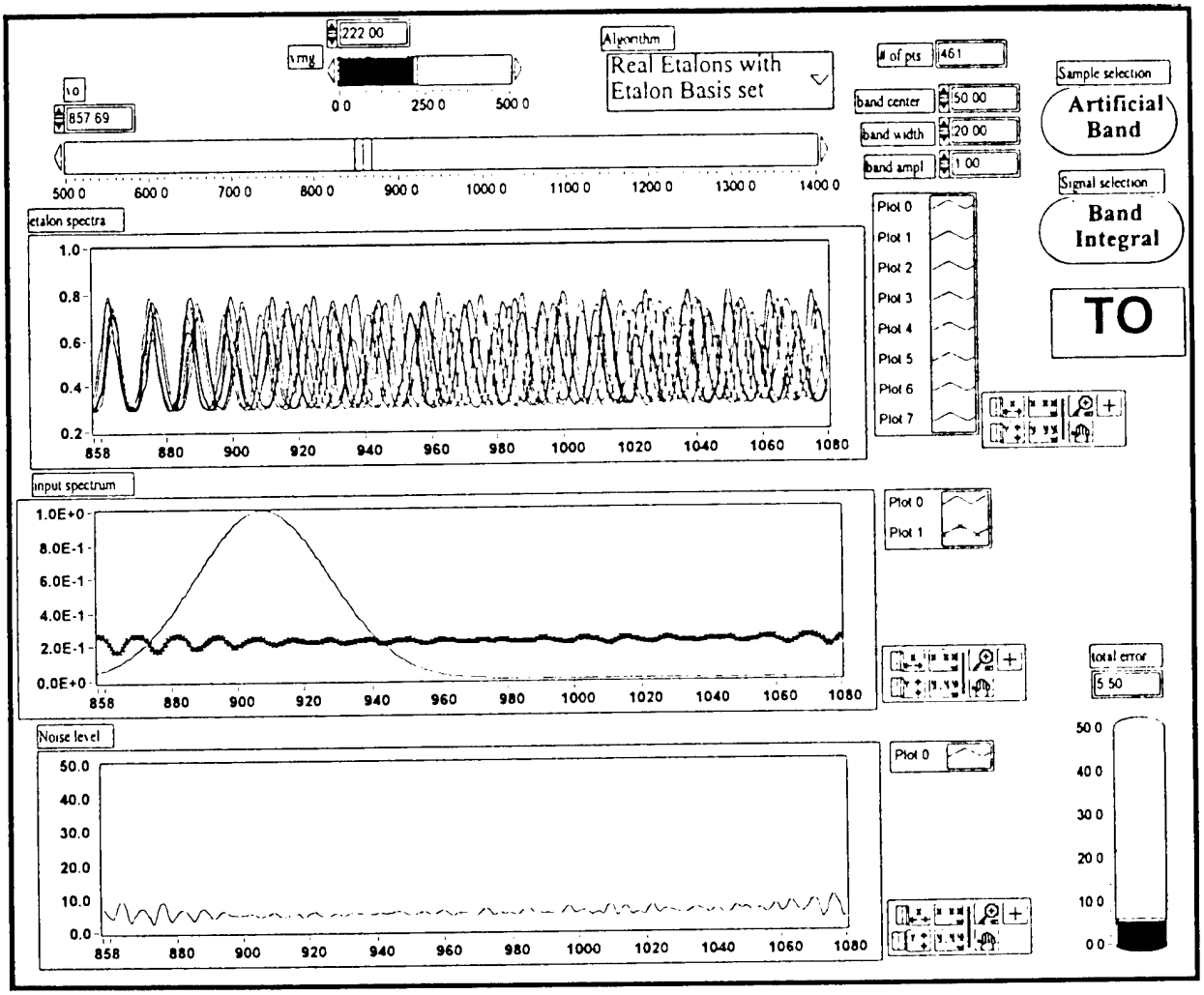

Figure 28. LabView Simulations of Etalon Set Containing only Thick Etalons, showing that broad features are not detected at all.

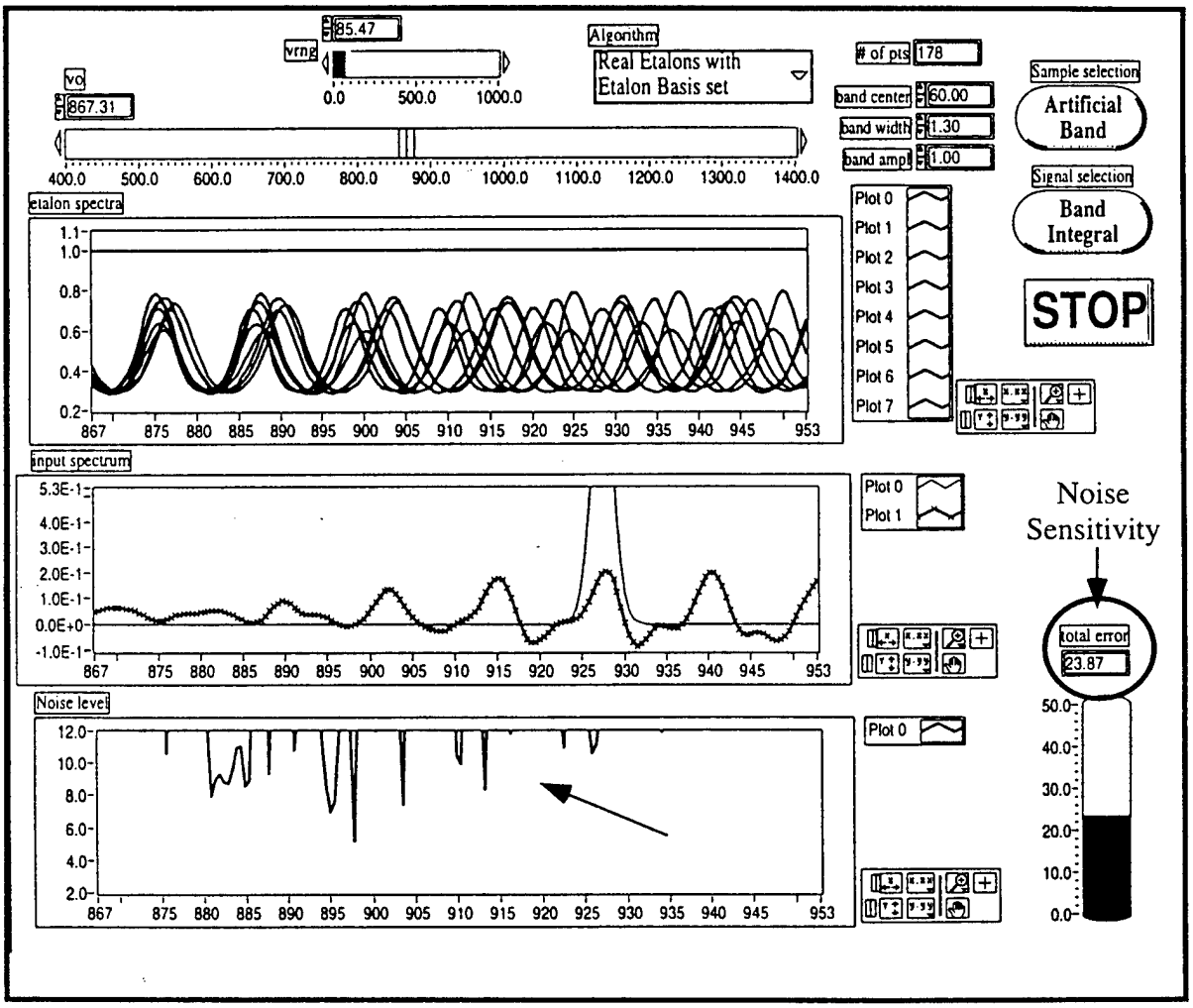

Figure 29. LabView Simulations of Etalon Set Containing only Thick Etalons, showing that inadequate bandwidth increases noise sensitivity.

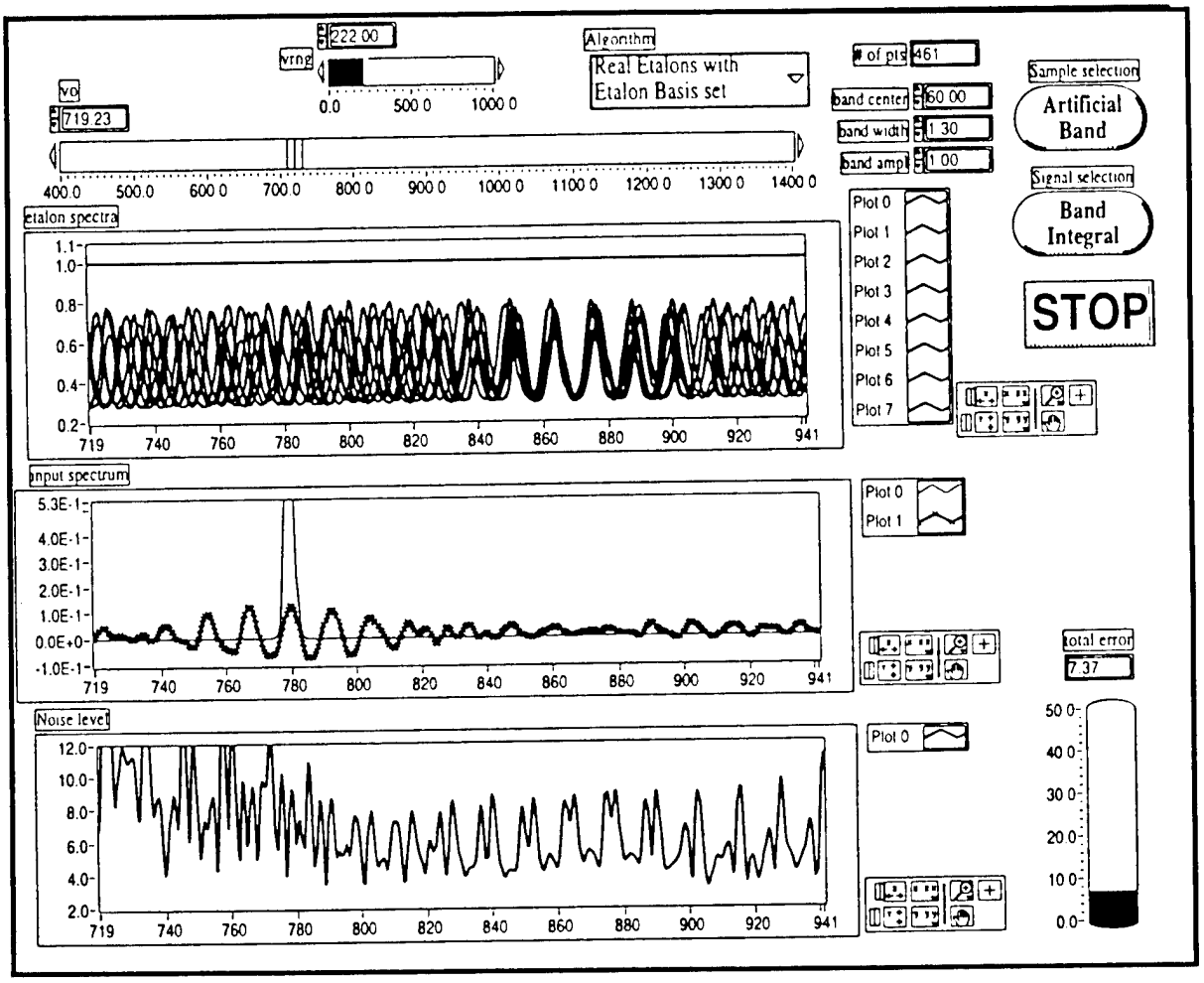

Figure 30. LabView Simulations of Etalon Set Containing only Thick Etalons, showing that center frequency of bandpass is important.

Graph A

Graph B

Graph C

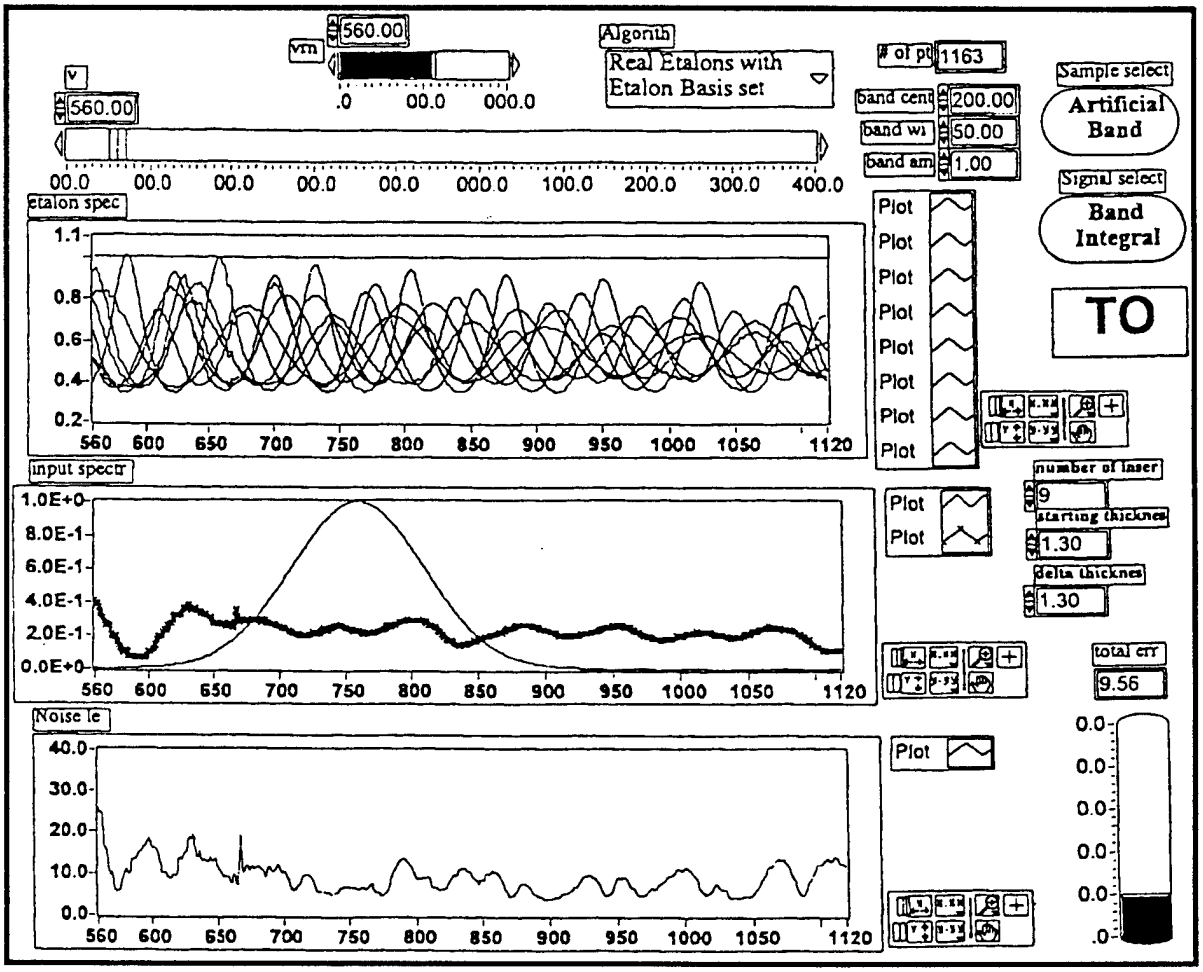

Figure 31. LabView Simulations of Etalon Set Containing Thinner Etalons (set T5), showing that broad features cannot be detected without the thinnest etalons.

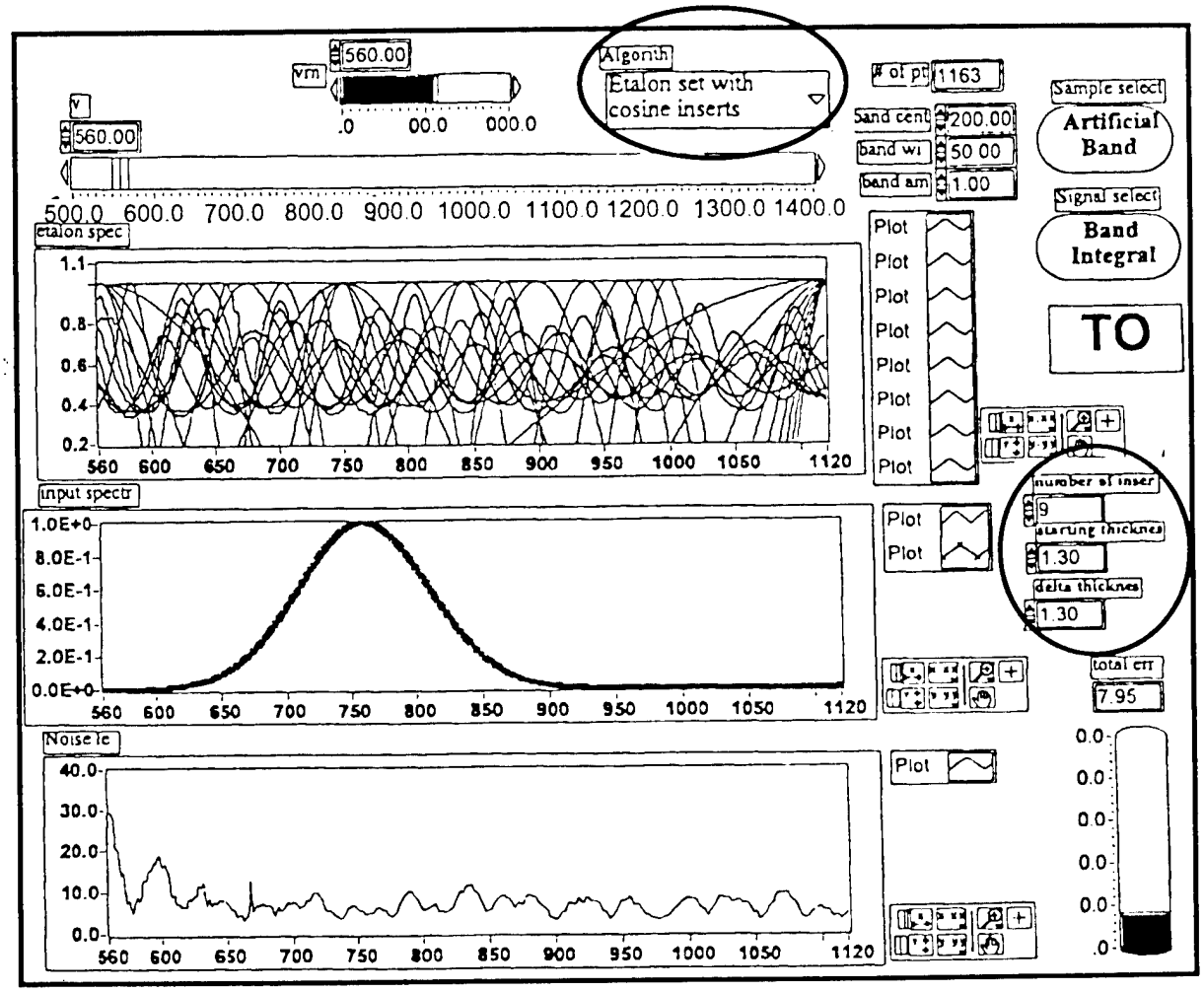

Figure 32. LabView Simulations of Etalon Set Containing Thinnest Etalons (set T7), showing that with (simulated) thin etalons, broad features are detected well.

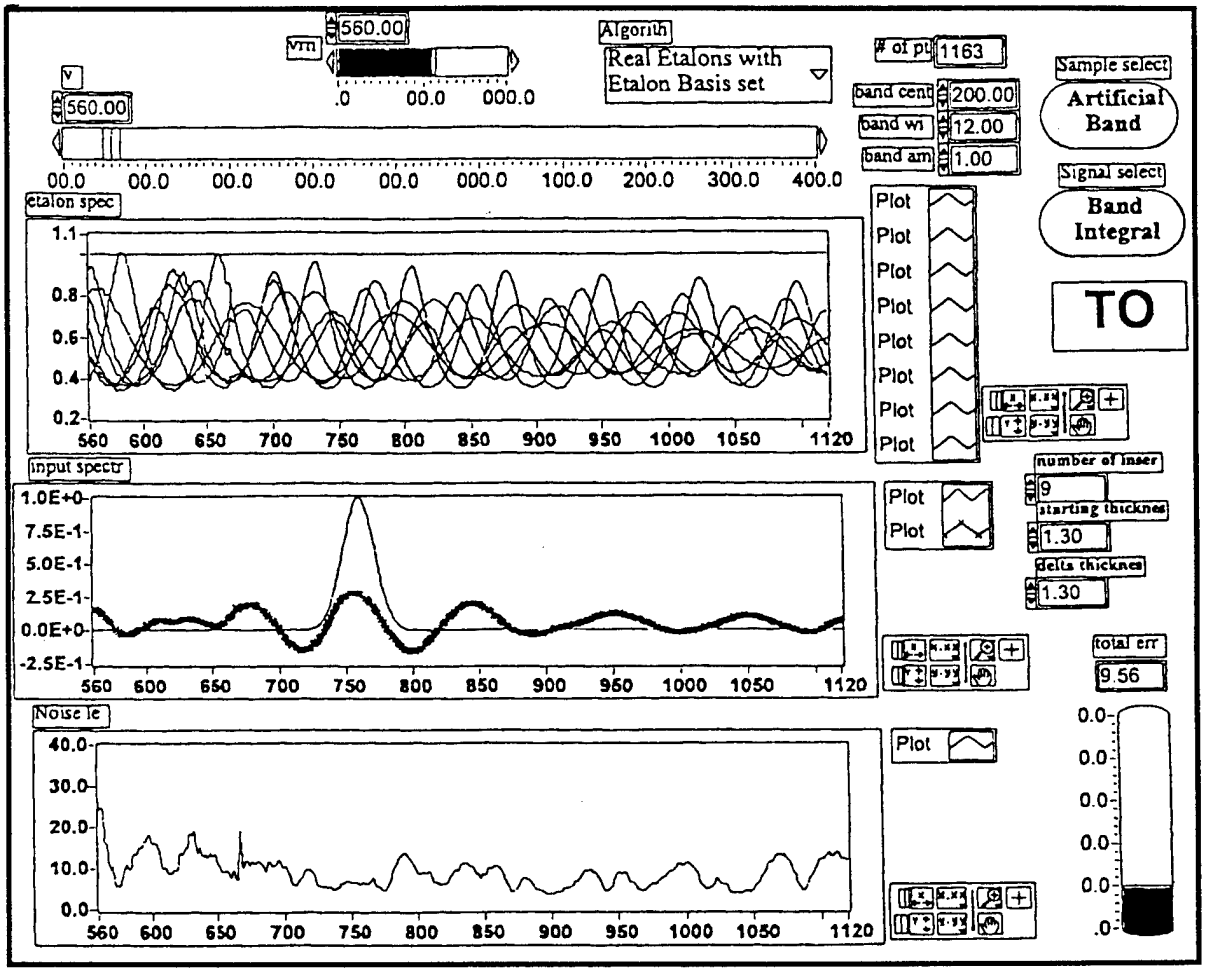

Figure 33. LabView Simulations of Etalon Set Containing Thinnest Etalons (set T5), showing that narrow features can be detected.

Graph A

Graph B

Graph C

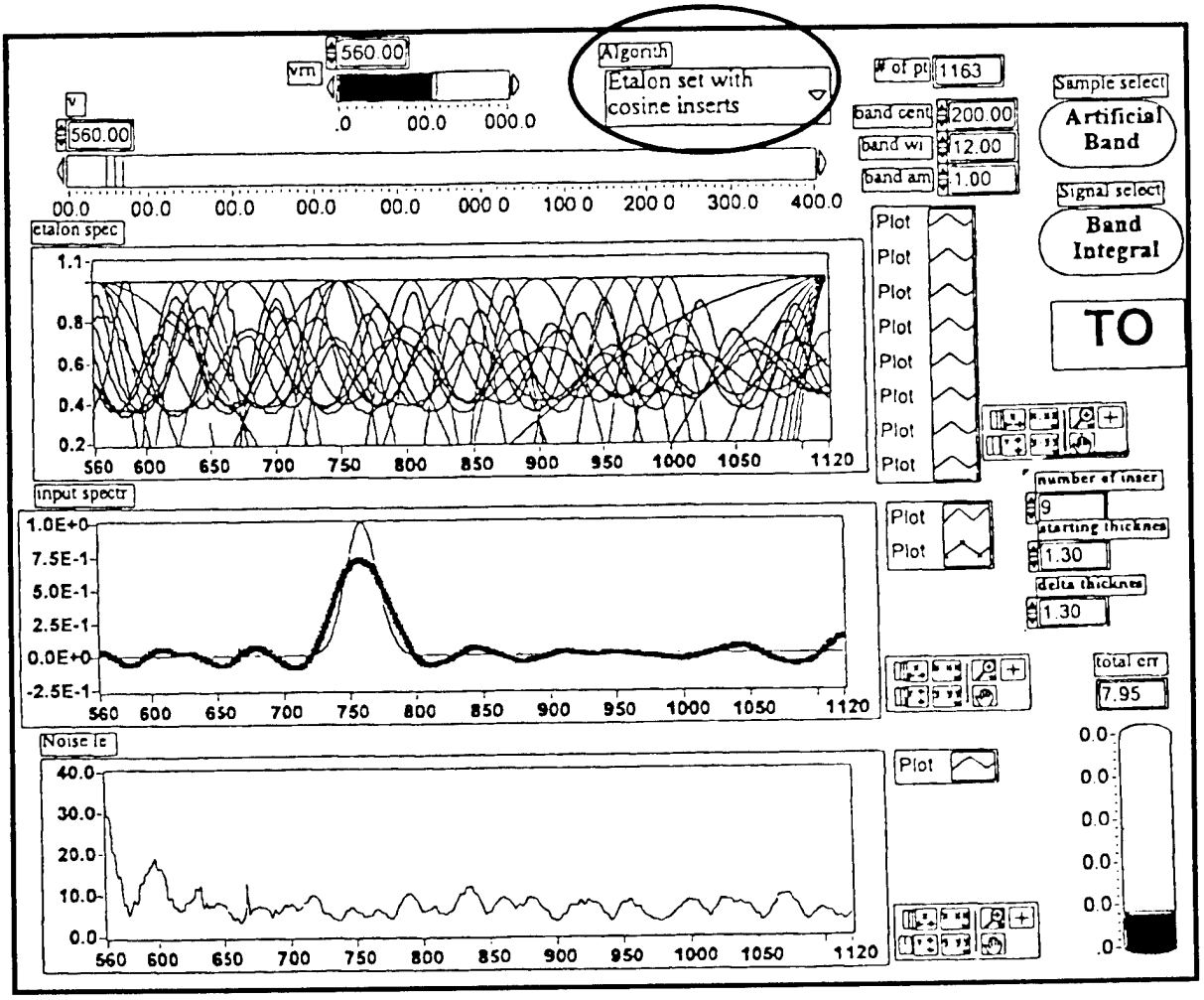

Figure 34. LabView Simulations of Etalon Set Containing Thinner Etalons (set T7), showing that (simulated) thin etalons improve the fit to narrow features.

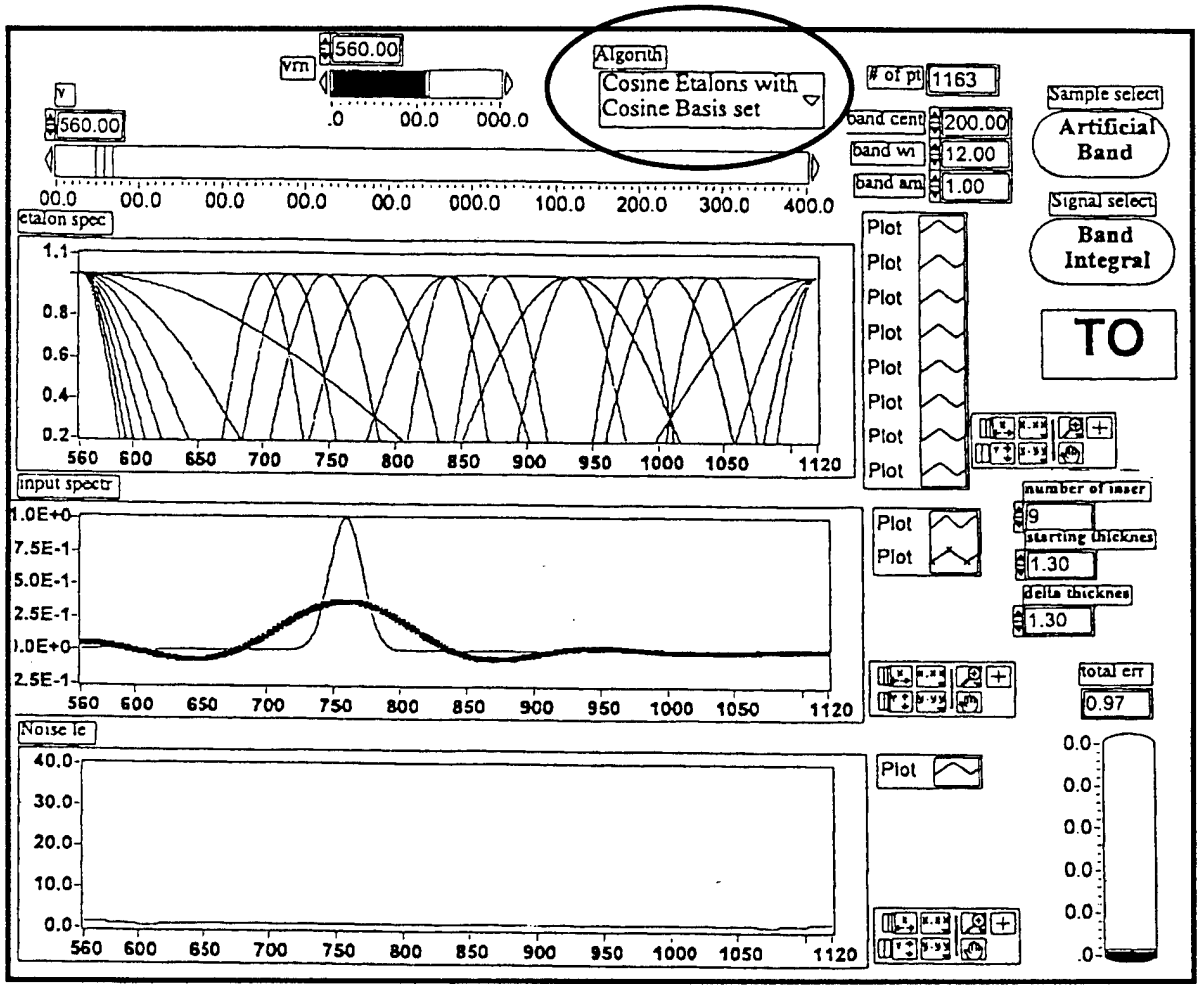

Figure 35. LabView Simulations of Etalon Set Containing only the thin simulated etalons, showing the fit to a thin feature.

Appendix B: Tables

Table I - Possible Etalon Sets
Each Etalon covers a Multiple of 5 channels

channels/etalon	Gap	Active	# of etalons	Total Active SuperPixels	Total Wasted
25	3	22	5	110	18
20	3	17	6	102	26
15	3	12	8	96	32
10	2	8	12	96	32
5	2	3	25	75	53

TABLE II

LITHOGRAPHY DESIGN RULES

Mask Layer Items: (sequentially, from first drawings to final fabricated device)
a) CAD file soft drawing, b) paper mask (in reversal),
c) photomask (reduced size), d) patterned photoresist mask, e) etched film.

Basic Guides and Limitations (Design Rules) :

1. Wafer substrate chips (e.g., silicon) must be **11x11 or 17x17** (±0.5) mm^2
2. Photomasks are contact printed at **1:1** into 1.2- m thick photoresist (*Shipley* 1400-25).
3. Minimum feature size (**MFS**) is **5 m**. This is minimum final-dimension width for both etched conducting films or gaps between film areas. This limit is set by trade-offs in laser printer and Rayleigh-limit of the lens aperture (f-stop). Use this as CAD grid size. *Caution*, actual microstructures will suffer roughly 50% yield at 5 m, so use 10 m or greater MFS rules for higher practical robustness.
4. All sizes greater than MFS will be **only integer multiples** of MFS. This is required by laser-printer line widths, which are integer multiples (i.e., digital).
5. Maximum usable area (**MUA**) for the device *and* its contact pads is ~**9x9** mm^2.
6. Put alignment cross hairs into each corner (exactly 8x8 mm^2) for printing into resist.
7. the margins on photomask must have a clear field ~14x14 or 20x20 mm^2, to allow for visual alignment of the mask (~1 mm off-center misalignment of mask and wafer centers).
8. For multi-layer masks, any critical overlap or gap margins must be a minimum of ~25 m (after reduction), to allow visual alignment of mask layers and overlap registry.
9. Photographic masks are **reductions of 20:1**. Photomasks are *Kodak* SO343 sheet film, with resolution of 1000 lines/mm. *Nikon* (35-mm roll film) camera and 50-mm lens are used (green filter optional). Typically, use four 150-W flood lamps for illumination.
10. Original paper masks are printed on ***HP*4-600dpi** laser printer, using special high-gloss and ultra-white paper. Add mat-black-paper boarders to give clear-field margins in the photomask (for alignment). Note that drawing on paper is 20x larger than final mask.

Paper masks are drawn with computer CAD (PC or MAC). Check line widths in trial prints of the paper-masks using measuring microscope. Lines or edges of shapes that are not horizontal or vertical will be drawn by the laser printer as stepped edges and smoothed by diffraction and abberation effects in the camera lens.

TABLE III

Etching Procedure for GIF Arrays Using MCNC nitride coated Si Wafers

I. Prethin MCNC nitride.

a). Soap clean + Standard RCA clean, leaves stable oxide coating: all in hot (~65°C) Ultrasound 5 sec, 5 minute soak, followed by 5 sec ultrasound for each of the following steps:

i) soap
ii) water
iii) piranha (4:1 recipe)
iv) water
v) SC-1
vi) water
vii) SC-2
viii) water (flush many times)

b) Coat Backside of wafer with paraffin Wax (90°C on hot plate)
c) Etch in room T 49% HF for ~1 hour, until pale yellow, goes through 3 cycles of blue.
d) Clean wax (all steps 5 minutes):
i) acetone at 65°C to remove wax, rinse several times
ii) IPA to remove acetone residue
iv) ethanol
v) dry
vi) hot piranha (5sec ultrasound, 5 minute soak, 5 sec ultrasound)
vii) hot DI (5 sec ultrasound, 5 minute soak, 5 sec ultrasound)
viii) dry

II. Print Mask

a) Bake 200°C for 30 minutes
b) Spin-on resist
c). Soft bake (1 minute, 90°C)
d). Align Mask and clamp contact, and expose 20 seconds
e). Develop 40 seconds in CD30.
f). Wash 30 seconds in DI
g). Hard Bake (15 minutes, 110°C), and cool 1-2 min.
h). Etch in 7:1 BOE (5 minutes, 65°C) w/o stirring
i). Strip and clean
i) acetone (room T 1-2 minutes)
ii) mini- RCA (like RCA above, but room T, 1 minute on all steps)
(piranha, water, SC-1, water, SC-2, water)

III. Etch Pit

a) 30-90 seconds in 90°C KOH (time depends on required depth)

Repeat step II with next mask.

Table IV. Specifications of Bolometer Array #512.

Detector Channel	Board Pin #	Resistance (kohms)	Signal @1.3mW/cm^2 (mVolts)	Pixel Responsivity (W/cm^2)	Noise (uV/rootHz @ 1Hz)	Remarks
1	55	4.87				Dead Channel
2	54	906	48.4	4.38E+05	452	
3	53	1770	48.7	4.41E+05	1.79	
4	52	1760	48.1	4.35E+05	1.81	
5	51	1800	47.7	4.32E+05	1.65	
6	50	1800	47.8	4.33E+05	1.83	
7	49	1800	48.1	4.35E+05	2.09	
8	48	1760	48.1	4.35E+05	2.1	
9	47	1590	47.1	4.26E+05	1.72	
10	46	1760	46.8	4.24E+05	1.62	
11	45	1750	45.8	4.14E+05	1.83	
12	44	1270	46.9	4.24E+05	1.59	
13	43	1800	46.7	4.23E+05	1.74	
14	42	1470	44.1	3.99E+05	449	High noise
15	41	1590	45.2	4.09E+05	6.92	
16	40	1750	45.7	4.14E+05	2.12	
17	39	1750	45.5	4.12E+05	1.76	
18	38	1580	44.6	4.04E+05	31	High noise
19	37	4.68				Dead Channel
20	36	1080	46.1	4.17E+05	28.5	High noise
21	35	1800	44.2	4.00E+05	1.63	
22	34	1580	43.3	3.92E+05	2.86	
23	33	5.29				Dead Channel
24	32	1220	43.3	3.70E+05	1.98	
25	31	1570	41.4	3.54E+05	2.22	

EACH CHANNEL IS A (78 IN PARALLEL) X (10 IN SERIES) SUPERPIXEL ARRAY
Flux=1.3mW/cm^2
Wavelength=8-12um
Vbias=10V

Table V. Specifications of Bolometer Array #570.

Detector Channel	Board Pin #	Resistance (kohms)	Signal @1.3mW/cm^2 (mVolts)	Pixel Responsivity (W/cm^2)	Noise (uV/rootHz @ 1Hz)	Remarks
1	55	1320	43.00	3.89E+05	1.77	
2	54	895	43.10	3.90E+05	1.46	
3	53	1330	42.80	3.87E+05	1.68	
4	52	1190	42.40	3.84E+05	1.42	
5	51	1490	42.30	3.83E+05	1.67	
6	50	1180	42.60	3.86E+05	1.74	
7	49	1300	41.60	3.76E+05	1.93	
8	48	1510	41.10	3.72E+05	1.83	
9	47	1350	42.00	3.80E+05	1.54	
10	46	1350	42.10	3.81E+05	1.76	
11	45	1200	41.50	3.76E+05	2.05	
12	44	1490	40.90	3.70E+05	1.73	
13	43	1360	41.80	3.78E+05	1.52	
14	42	870	40.70	3.68E+05	1.62	
15	41	1360	40.80	3.69E+05	1.72	
16	40	1360	40.50	3.67E+05	1.57	
17	39	1370	40.90	3.70E+05	1.37	
18	38	1520	40.90	3.70E+05	1.67	
19	37	1370	40.40	3.66E+05	1.50	
20	36	1340	40.90	3.70E+05	1.34	
21	35	1370	41.70	3.77E+05	1.81	
22	34	1380	40.00	3.62E+05	1.74	
23	33	1.75				Shorted
24	32	1090	40.10	3.63E+05	1.70	
25	31	1560	38.90	3.52E+05	2.10	
Common	30,56					

EACH CHANNEL IS A 78 PARALLEL X 10 SERIES SUPERPIXEL ARRAY
Flux=1.3mW/cm^2
Wavelength=8-12um
Vbias=10V

Table VI - Etalon Sizes for Simulations								
Etalon #	0	1	2	3	4	5	6	7
Actual Size	0.00	4.84	10.00	16.60	21.90	24.15	28.99	33.82
Target Size	0.00	4.83	9.66	14.49	19.32	24.15	28.99	33.82
% difference	0.00	-0.21	-3.52	-14.56	-13.35	0.00	0.00	0.00

Table VII Raw Signals from Bolometer Channels					
Data on GIF's from 5/14/98					
Signals in micro-volts, after G 100 preamp.					
Bias current = 5.6v					
Detector #					
	1	2	3	4	5
none	631.0	710.0	781.0	693.0	560.1
Broad	37.2	52.9	63.2	55.9	44.2
Narrow	19.3	27.4	33.1	29.5	23.1
Bias current = 10.0v					
Etalon #4	**Detector #**				**thinnest**
	1	2	3	4	5
none	833.0	981.0	1098.0	971.0	777.0
Broad	40.0	62.1	73.7	64.1	49.4
Narrow	20.3	31.7	38.0	33.8	26.4
Both	17.5	27.0	31.7	28.5	22.3
Bias current = 10.0v					
Etalon #5	**Detector #**				
	1	2	3	4	5
none	815.0	965.0	1070.0	936.0	721.0
Broad	37.6	58.9	71.0	61.0	45.3
Narrow	20.7	31.6	36.2	32.1	23.6
Both	16.0	25.5	30.1	26.8	19.5

Table VIII - Signal Correction Factors				
Signal correction factor				
1.24	1.10	1.00	1.13	1.39
1.70	1.19	1.00	1.13	1.43
1.72	1.21	1.00	1.12	1.43

Table IX - Corrected Signal					
	1	2	3	4	5
none	1450.0	1450.0	1450.0	1450.0	1450.0
Broad	119.0	119.0	119.0	119.0	119.0
Narrow	62.3	62.3	62.3	62.3	62.3
Bias current = 10.0v					
Etalon #4	**Detector #**				**thinnest**
	1	2	3	4	5
none	1023.6	1085.8	1098.0	1100.0	1079.2
Broad	68.0	74.0	73.7	73.3	71.0
Narrow	33.0	39.0	38.0	38.3	37.4
Both	28.5	33.2	31.7	32.3	31.6
Bias current = 10.0v					
Etalon #5	**Detector #**				**Thickest**
	1	2	3	4	5
none	1001.5	1068.1	1070.0	1060.3	1001.4
Broad	63.4	71.0	71.0	69.1	64.7
Narrow	34.9	38.1	36.2	36.3	33.7
Both	27.0	30.8	30.1	30.3	27.9

AFRL-SR-BL-TR-98-

0594

REPORT DOCUMENTATION PAGE

1. AGENCY USE ONLY *(Leave blank)*	2. REPORT DATE	3. REPORT TYPE AND DATES COVERED
	8/15/98	Final Report: 8/15/97 – 5/14/98

6. TITLE AND SUBTITLE
Infrared Spectrometer on a Chip

7. FUNDING NUMBERS
F49620-97-C-0050

8. AUTHORS
David G. Hamblen

9. PERFORMING ORGANIZATION NAME(S) AND ADDRESS(ES)
Advanced Fuel Research, Inc.
87 Church Street
East Hartford, CT 06108-3742

10. PERFORMING ORGANIZATION REPORT NUMBER
526048

11. SPONSORING/MONITORING AGENCY NAME(S) AND ADDRESS(ES)
Air Force Office at Scientific Research
110 Duncan Avenue, Suite B115
Bolling AFB, DC 20332-8080

10. SPONSORING/MONITORING AGENCY REPORT NUMBER
0002AA 8/14/98

11. SUPPLEMENTARY NOTES

12a. DISTRIBUTION/AVAILABILITY STATEMENT
Distribution Statement A – Approved for pubic release; distribution is unlimited

12b. DISTRIBUTION CODE
A

12. ABSTRACT *(Maximum 200 words)*

Applications for infrared spectroscopy appear in the semiconductor, utility, petroleum, chemical, transportation, medical and environmental industries, in R&D and in the military. The drawback is that infrared spectrometers and detectors are complex systems which are expensive ($20,000 or more) and involve moving mechanical parts which must be maintained in careful alignment. There is a need for low-cost (less than a few hundred dollars) devices which can be used in these applications. This Phase I project has successfully demonstrated the combination of Advanced Fuel Research's graded-interference-filter (GIF) spectrometer and Raytheon/TI Systems' a-Si microbolometer arrays. During the course of this project, we have fabricated 3 etalon sets, suitable for mating with the microbolometers. Two 256x78 microbolometer arrays were fabricated by Raytheon, wired internally into 25 channels of 10x78 pixels each. These etalon/microbolometer arrays were tested successfully in a spectrometer/test fixture. This spectrometer includes an infrared source, focusing optics, provision for a gas cell, micromanipulators for the etalon and microbolometer arrays, biasing and signal conditioning electronics, and a chopper/modulator for the bolometers. Several design variations were evaluated using a LabView computer program: incomplete etalon sets, etalons sets with thicknesses differing from the design target thicknesses, and the effect of differing bandpass filters in the optical path.

13. SUBJECT TERMS

15. NUMBER OF PAGES
62

16. PRICE CODE

17. SECURITY CLASSIFICATION OF REPORT	18. SECURITY CLASSIFICATION OF THIS PAGE	19. SECURITY CLASSIFICATION OF ABSTRACT	20. LIMITATION OF ABSTRACT
Unclassified	Unclassified	Unclassified	Unclassified

NSN 7540-01-280-5500 Computer Generated STANDARD FORM 298 (Rev 2-89)
Prescribed by ANSI Std 239-18
298-102